20

Wideband Representation of Passive Components based on Planar Waveguide Junctions

Fermín Mira[1], Ángel A. San Blas[2], Vicente E. Boria[3] and Benito Gimeno[4]
[1]*Centre Tecnològic de Telecomunicacions de Catalunya (CTTC),*
[2]*Universidad Miguel Hernández de Elche,*
[3]*iTEAM - Universidad Politécnica de Valencia,*
[4]*ICMUV-Universidad de Valencia,*
Spain

1. Introduction

Modern microwave and millimeter-wave equipment, present in mobile, wireless and space communication systems, employ a wide variety of waveguide components (Uher et al., 1993; Boria & Gimeno, 2007). Most of these components are based on the cascade connection of waveguides with different cross-section (Conciauro et al., 2000). Therefore, the full-wave modal analysis of such structures has received a considerable attention from the microwave community (Sorrentino, 1989; Itoh, 1989). The numerical efficiency of these methods has been substantially improved in (Mansour & MacPhie, 1986; Alessandri et al., 1988; Alessandri et al., 1992) by means of the segmentation technique, which consists of decomposing the analysis of a complete waveguide structure into the characterization of its elementary key-building blocks, i.e. planar junctions and uniform waveguides.
The modeling of planar junctions between waveguides of different cross-section has been widely studied in the past through modal analysis methods, where higher-order mode interactions were already considered (Wexler, 1967). For instance, in order to represent such junctions, the well-known mode-matching technique has been typically formulated in terms of the generalized scattering matrix (Safavi-Naini & MacPhie, 1981; Safavi-Naini & MacPhie, 1982; Eleftheriades et al., 1994). Alternatively, the planar waveguide junction can be characterized using a generalized admittance matrix or a generalized impedance matrix, obtained either by applying the general network theory (Alvarez-Melcón et al., 1996) or by solving integral equations (Gerini et al., 1998). A common drawback to all the previous techniques is that any related generalized matrix must be recomputed at each frequency point.
In the last two decades, several works have been focused on avoiding the repeated computations of the cited generalized matrices within the frequency loop. For instance, frequency independent integral equations have been set up when dealing, respectively, with inductive (or H-plane) and capacitive (or E-plane) discontinuities (Guglielmi & Newport,

1990; Guglielmi & Alvarez-Melcón, 1993), steps (Guglielmi et al., 1994; Guglielmi & Gheri, 1994), and posts (Guglielmi & Gheri, 1995). On the other hand, following the Boundary Integral-Resonant Mode Expansion (BI-RME) technique developed at the University of Pavia (Italy), a generalized admittance matrix in the form of pole expansions has been derived for arbitrarily shaped H-plane (Conciauro et al., 1996) and E-plane components (Arcioni et al., 1996), as well as for 3-D resonant waveguide cavities (Arcioni et al., 2002).
The objective of this chapter will be to describe a new method for the analysis of passive waveguide components, composed of the cascade connection of planar junctions. This new method extracts the main computations out of the frequency loop, thus reducing the overall CPU effort for solving the frequency-domain problem. The key points to reach such objectives are:

- Starting from the integral equation technique for the representation of planar waveguide junctions (Gerini et al., 1998), we propose a novel formulation of the generalized impedance and admittance matrices in the form of quasi-static terms and a pole expansion. A convergence study of this novel algorithm will be presented, where the two formulations in form of impedance and admittance matrices are compared in terms of efficiency and robustness.
- Once the generalized matrices of planar junctions are expressed in the form of pole expansions, a novel technique that provides the wideband generalized impedance or admittance matrix representation of the whole structure in the same form will be presented. For this purpose, the structure is segmented into planar junctions and uniform waveguide sections, which are both characterized in terms of wideband impedance/admittance matrices. Then, an efficient iterative algorithm for combining such matrices, and finally providing the wideband generalized impedance matrix of the complete structure, is followed (Arcioni & Conciauro, 1999). A special formulation will be derived for two-dimensional structures in order to obtain more optimized algorithms for this kind of geometries widely employed in practical designs.

Finally, the proposed method will be validated though the presentation of several practical designs. The results provided by our novel method will be compared with those provided by the previous methods commonly employed for the analysis of such passive devices, as well as with the results provided by commercial software.

2. Generalized *Z* and *Y* matrices of Planar Waveguide Steps

The structure under study is the planar junction between two arbitrarily shaped waveguides shown in Fig. 1. Following the integral equation technique described in (Gerini et al., 1998), such junction can be represented in terms of a generalized Z or Y matrix, and two sets of asymptotic modal admittances or impedances (see Fig. 1), which are determined as follows

$$\hat{Y}_m^{(\delta)} = \lim_{m\to\infty} Y_m^{(\delta)} = \begin{cases} \kappa_m^{(\delta)} / (jk\eta) & \text{TE modes} \\ jk / (\kappa_m^{(\delta)}\eta) & \text{TM modes} \end{cases} \tag{1}$$

$$\hat{Z}_m^{(\delta)} = \lim_{m\to\infty} \left(1 / Y_m^{(\delta)}\right) = \begin{cases} jk\eta / \kappa_m^{(\delta)} & \text{TE modes} \\ \kappa_m^{(\delta)}\eta / (jk) & \text{TM modes} \end{cases} \tag{2}$$

where $Y_m^{(\delta)}$ represents the modal admmitance of the m-th mode at at waveguide port δ (δ=1,2)

$$Y_m^{(\delta)} = \begin{cases} \gamma_m / (jk\eta) & \text{TE modes} \\ jk / (\gamma_m \eta) & \text{TM modes} \end{cases} \qquad \gamma_m = \sqrt{\kappa_m^{(\delta)} - k^2} \tag{3}$$

and $\kappa_m^{(\delta)}$ is the cutoff wavenumber (Conciauro et al., 2000).

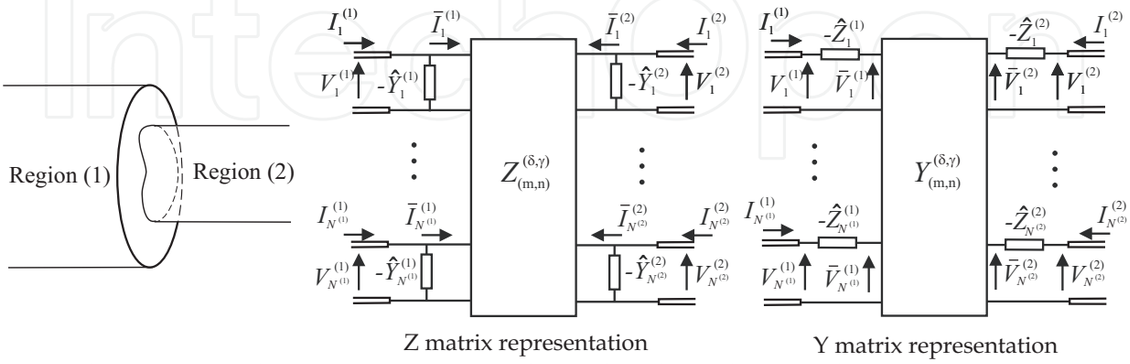

Fig. 1. Planar junction between two waveguides and multimode equivalent circuit representation in form of generalized Z and Y matrices.

2.1 Generalized *Z* matrix formulation

In order to derive the expressions for the elements of the generalized Z matrix of the planar junction (see Fig. 1), the next integral equation set up for the magnetic field at the junction plane must be solved (see more details about its derivation in (Gerini et al., 1998))

$$\mathbf{h}_n^{(\gamma)}(s) = \int_{S^{(2)}} \sum_{\zeta=1}^{2} \left[\sum_{m=1}^{\infty} \hat{Y}_m^{(\zeta)} \mathbf{h}_m^{(\zeta)}(s) \mathbf{h}_m^{(\zeta)}(s') - \sum_{m=N^{(\zeta)}+1}^{\infty} \hat{Y}_m^{(\zeta)} \left(1 - \frac{Y_m^{(\zeta)}}{\hat{Y}_m^{(\zeta)}} \right) \mathbf{h}_m^{(\zeta)}(s) \mathbf{h}_m^{(\zeta)}(s') \right] \cdot \mathbf{M}_n^{(\gamma)}(s') ds' \tag{4}$$

where $\mathbf{h}_n^{(\gamma)}$ is the normalized magnetic field related to the n-th mode at waveguide γ (Conciauro et al., 2000), and $\mathbf{M}_n^{(\gamma)}$ is the unknown magnetic current related to the electric field at the junction plane

$$\mathbf{z} \times \mathbf{E} = \sum_{n=1}^{N^{(1)}} \bar{I}_n^{(1)} \mathbf{M}_n^{(1)} - \sum_{n=1}^{N^{(2)}} \bar{I}_n^{(2)} \mathbf{M}_n^{(2)} \tag{5}$$

If we want to find an expression for the Z matrix in the form of pole expansions, we must express the kernel of the previous integral equation as a sum of terms depending on k and $1/k$. Taking into account (1), the first summation of (4) fulfills such condition directly. Regarding the second summation in (4), since $Y_m^{(\zeta)} \to \hat{Y}_m^{(\zeta)}$ when $m \to \infty$, we can approximate the term within parenthesis by its Taylor series

$$\left(1 - \frac{Y_m^{(\zeta)}}{\hat{Y}_m^{(\zeta)}} \right) \approx \sum_{r=1}^{R} c_r \left(\frac{k}{\kappa_m^{(\zeta)}} \right)^{2r} \tag{6}$$

where the values of the first coefficients c_r for the TE and TM modes are shown in Table 1. Then, if we consider a k^2 frequency dependency for TE modes and all contributions from TM

modes are set to be frequency independent (due to the definitions of the asymptotic modal admittances given in (1) and the expression for the second summation in (4)), we can rewrite the previous Taylor series as follows

$$\left(1-\frac{Y_m^{(\zeta)}}{\hat{Y}_m^{(\zeta)}}\right)\approx\begin{cases}\left(\dfrac{k}{k_0}\right)^2\displaystyle\sum_{r=1}^{R}c_r\left(\frac{k_0}{\kappa_m^{(\zeta)}}\right)^{2r} & \text{TE}\\ \displaystyle\sum_{r=1}^{R}c_r\left(\frac{k_0}{\kappa_m^{(\zeta)}}\right)^{2r} & \text{TM}\end{cases} \tag{7}$$

where k_0 corresponds to the value of k at the center point of the frequency range. Proceeding in this way, we manage to express the second series of (4) as the required combination of terms with k and $1/k$ dependence. By introducing the value of k_0 into (7), we reduce the number of accessible modes $N^{(\gamma)}$ required to obtain an accurate representation of the planar junction in the whole frequency range.

r	TE (Z matrix) TM (Y matrix)	TM (Z matrix) TE (Y matrix)
1	1/2	-1/2
2	1/8	-3/8
2	1/16	-5/16

Table 1. Values of the first coefficients c_r for TE and TM modes.

Then, making use of eqs. (1) and (7) into (4) , we can easily obtain the next integral equation

$$\begin{aligned}\mathbf{h}_n^{(\gamma)}(s)=\int_{S^{(2)}}\sum_{\zeta=1}^{2}\Bigg[&\frac{1}{jk\eta}\sum_{m^{TE}=1}^{\infty}\kappa_m^{(\zeta)}\mathbf{h}_m^{(\zeta)}(s)\mathbf{h}_m^{(\zeta)}(s')+\frac{jk}{\eta}\Bigg(\sum_{m^{TM}=1}^{\infty}\frac{\mathbf{h}_m^{(\zeta)}(s)\mathbf{h}_m^{(\zeta)}(s')}{\kappa_m^{(\zeta)}}\\&+\sum_{m^{TE}=N^{(\zeta)}+1}^{\infty}\mathbf{h}_m^{(\zeta)}(s)\mathbf{h}_m^{(\zeta)}(s')\sum_{r=1}^{R}\frac{c_r k_0^{2r-2}}{\left(\kappa_m^{(\zeta)}\right)^{2r-1}}-\sum_{m^{TM}=N^{(\zeta)}+1}^{\infty}\mathbf{h}_m^{(\zeta)}(s)\mathbf{h}_m^{(\zeta)}(s')\sum_{r=1}^{R}\frac{c_r k_0^{2r}}{\left(\kappa_m^{(\zeta)}\right)^{2r+1}}\Bigg)\Bigg]\cdot\mathbf{M}_n^{(\gamma)}(s')ds'\end{aligned} \tag{8}$$

where the original summations in m have been divided into the contributions of TE (m^{TE}) and TM (m^{TM}) modes.

Now, we can solve the previous integral equation by means of the Method of Moments (MoM). Expanding the unknown magnetic current in terms of the modes of the waveguide with a smaller cross-section (note that $\mathbf{z}\times\mathbf{E}=0$ out of the intersection of the two waveguides)

$$\mathbf{M}_n^{(\gamma)}(s')=\sum_{q=1}^{Q}\alpha_{q,n}^{(\gamma)}\,\mathbf{h}_q^{(2)}(s') \tag{9}$$

and using the Galerkin approach, we finally obtain the following linear system of equations

$$\mathbf{P}\cdot\boldsymbol{\alpha}^{(\gamma)}=\mathbf{Q}^{(\gamma)} \tag{10}$$

where $\boldsymbol{\alpha}^{(\gamma)}$ contains the unknown coefficients $\alpha_{q,n}^{(\gamma)}$, whereas $\mathbf{Q}^{(\gamma)}$ and $\mathbf{P}$ matrix elements are computed as indicated next

$$Q_{p,n}^{(\gamma)} = \int_{S^{(2)}} \mathbf{h}_p^{(2)}(s)\,\mathbf{h}_n^{(\gamma)}(s)\,ds = \begin{cases} \sigma_{p,n} & (\gamma)=(1) \\ \delta_{p,n} & (\gamma)=(2) \end{cases} \tag{11}$$

$$\mathbf{P} = \frac{1}{jk\eta}\left(\mathbf{R} - k^2\mathbf{S}\right) \tag{12}$$

$$R_{p,q} = \sum_{m^{TE}=1}^{\infty} \kappa_m^{(1)} \sigma_{p,m}\,\sigma_{q,m} + \kappa_p^{(2)}\delta_{p,q}^{TE} \tag{13}$$

$$\begin{aligned} S_{p,q} = & \frac{\delta_{p,q}^{TM}}{\kappa_p^{(2)}} + \sum_{m^{TM}=1}^{\infty} \frac{\sigma_{p,m}\sigma_{q,m}}{\kappa_m^{(1)}} + F_p\left(\delta_{p,q}^{TE} - \left(\frac{k_0}{\kappa_p^{(2)}}\right)^2 \delta_{p,q}^{TM}\right)\sum_{r=1}^{R} \frac{c_r k_0^{2r-2}}{\left(\kappa_p^{(2)}\right)^{2r-1}} \\ & + \sum_{m^{TE}=N^{(1)}+1}^{\infty} \sigma_{p,m}\sigma_{q,m} \sum_{r=1}^{R} \frac{c_r k_0^{2r-2}}{\left(\kappa_m^{(1)}\right)^{2r-1}} - \sum_{m^{TM}=N^{(1)}+1}^{\infty} \sigma_{p,m}\sigma_{q,m} \sum_{r=1}^{R} \frac{c_r k_0^{2r}}{\left(\kappa_m^{(1)}\right)^{2r+1}} \end{aligned} \tag{14}$$

where $\delta_{p,q}$ stands for the Kronecker's delta (i.e. $\delta_{p,q}=1$ if $p=q$ and $\delta_{p,q}=0$ if $p\neq q$), and

$$F_p \equiv \begin{cases} 0 & p < N^{(2)}+1 \\ 1 & p \geq N^{(2)}+1 \end{cases} \tag{15}$$

It is interesting to see that **R** and **S** can be expressed as the following block matrices

$$\mathbf{R} = \begin{bmatrix} \mathbf{R}_{11} & \mathbf{0}_{12} \\ \mathbf{0}_{21} & \mathbf{0}_{22} \end{bmatrix} \quad \mathbf{S} = \begin{bmatrix} \mathbf{S}_{11} & \mathbf{S}_{12} \\ \mathbf{S}_{21} & \mathbf{S}_{22} \end{bmatrix} \tag{16}$$

where the subscript 1 corresponds with the TE modes, and the subscript 2 with the TM modes, used in (9). Notice that the elements $R_{p,q}$ are zero whenever p or q are related to TM modes, since the coupling coefficients $\sigma_{p,m}$ are zero when p is a TM mode and m is a TE mode (Guillot et al., 1993). Therefore, the matrix **P** can be written as

$$\mathbf{P} = \frac{1}{jk\eta}\begin{bmatrix} \mathbf{R}_{11} - k^2\mathbf{S}_{11} & -k^2\mathbf{S}_{12} \\ -k^2\mathbf{S}_{12}^T & -k^2\mathbf{S}_{22} \end{bmatrix} \tag{17}$$

For solving the linear system defined in (10), the **P** matrix must be inverted. Following (Zhang, 1999), we can say that

$$\mathbf{P}^{-1} = jk\eta\begin{bmatrix} \mathbf{P}_{11}^{-1} & -\mathbf{P}_{11}^{-1}\mathbf{S}_{12}\mathbf{S}_{22}^{-1} \\ -\mathbf{S}_{22}^{-1}\mathbf{S}_{12}^T\mathbf{P}_{11}^{-1} & \mathbf{S}_{22}^{-1}\mathbf{S}_{12}^T\mathbf{P}_{11}^{-1}\mathbf{S}_{12}\mathbf{S}_{22}^{-1} - \mathbf{S}_{22}^{-1}/k^2 \end{bmatrix} \tag{18}$$

where $\mathbf{P}_{11} = \mathbf{R}_{11} - k^2(\mathbf{S}_{11} - \mathbf{S}_{12}\mathbf{S}_{22}^{-1}\mathbf{S}_{12}^T)$. The inverse of this block can be easily obtained after solving the generalized eigenvalue problem shown next

$$\mathbf{R}_{11}\mathbf{x} = k^2\left(\mathbf{S}_{11} - \mathbf{S}_{12}\mathbf{S}_{22}^{-1}\mathbf{S}_{12}^T\right)\mathbf{x} \tag{19}$$

If the matrix $\mathbf{X} = (\mathbf{x}_1, \mathbf{x}_2, \ldots, \mathbf{x}_{Q_1})$, whose Q_1 columns are the eigenvector solutions of the previous problem (Q_1 being the number of the total Q basis functions in (9) corresponding to TE modes), is normalized as follows

$$\mathbf{X}_T\mathbf{R}_{11}\mathbf{X} = \mathbf{\Lambda} = (k_1^2, k_1^2, \ldots, k_{Q_1}^2) \tag{20}$$

$$\mathbf{X}_T\left(\mathbf{S}_{11} - \mathbf{S}_{12}\,\mathbf{S}_{22}^{-1}\mathbf{S}_{12}^T\right)\mathbf{X} = \mathbf{U} = \mathrm{diag}(1,1,\ldots,1) \tag{21}$$

where k_i is the i-th eigenvalue solution of the previous problem, we can easily write that

$$\mathbf{P}_{11}^{-1} = \sum_{i=1}^{Q_1} \frac{\mathbf{x}_i\{\mathbf{x}_i\}^T}{k_i^2 - k^2} \tag{22}$$

Finally, if we extract the limit value of the previous summation when $k \to 0$, which is obviously equal to $\mathbf{R}_{11}^{-1}$, we obtain the following expression

$$\mathbf{P}_{11}^{-1} = \mathbf{R}_{11}^{-1} + k^2 \sum_{i=1}^{Q_1} \frac{\mathbf{x}_i\{\mathbf{x}_i\}^T}{k_i^2(k_i^2 - k^2)} \tag{23}$$

where the series in (23) converges with a very low number of terms, rather smaller than Q_1, due to the previous extraction of the low-frequency term in the matrix $\mathbf{P}_{11}^{-1}$.

Introducing now (23) into (18), we obtain the next expressions for the different blocks of the $\mathbf{P}^{-1}$ matrix

$$(\mathbf{P}^{-1})_{11} = jk\eta\mathbf{R}_{11}^{-1} + jk^3\eta \sum_{i=1}^{Q_1} \frac{\mathbf{x}_i\{\mathbf{x}_i\}^T}{k_i^2(k_i^2 - k^2)} \tag{24}$$

$$(\mathbf{P}^{-1})_{12} = -jk\eta\mathbf{R}_{11}^{-1}\mathbf{S}_{12}\mathbf{S}_{22}^{-1} - jk^3\eta \sum_{i=1}^{Q_1} \frac{\mathbf{x}_i\{\mathbf{x}_i'\}^T}{k_i^2(k_i^2 - k^2)} \tag{25}$$

$$(\mathbf{P}^{-1})_{22} = \frac{\eta}{jk}\mathbf{S}_{22}^{-1} + jk\eta\,\mathbf{S}_{22}^{-1}\mathbf{S}_{12}^T\mathbf{R}_{11}^{-1}\mathbf{S}_{12}\mathbf{S}_{22}^{-1} + jk^3\eta \sum_{i=1}^{Q_1} \frac{\mathbf{x}_i'\{\mathbf{x}_i'\}^T}{k_i^2(k_i^2 - k^2)} \tag{26}$$

where $\mathbf{x}_i' = \mathbf{S}_{22}^{-1}\mathbf{S}_{12}^T\mathbf{x}_i$. Once the $\mathbf{P}$ matrix has been successfully inverted, the elements of the generalized Z matrix of the planar step can be obtained through the evaluation of

$$Z_{m,n}^{(\delta,\gamma)} = \sum_{q=1}^{Q} \alpha_{q,n}^{(\gamma)} \int_{S^{(2)}} \mathbf{h}_q^{(2)}\,\mathbf{h}_m^{(\delta)}\,ds = \{\mathbf{Q}^{(\delta)}\}^T\,\mathbf{P}^{-1}\mathbf{Q}^{(\gamma)} \tag{27}$$

thus obtaining the following final expressions for all possible combinations of TE and TM modes

$$\mathbf{Z}_{\text{TE-TE}}^{(\delta,\gamma)} = jk\eta\{\mathbf{Q}_{11'}^{(\delta)}\}^T\,\mathbf{R}_{11}^{-1}\mathbf{Q}_{11'}^{(\gamma)} + jk^3\eta \sum_{i=1}^{Q_1} \frac{\mathbf{y}_i'^{(\delta)}\{\mathbf{y}_i'^{(\gamma)}\}^T}{k_i^2(k_i^2 - k^2)} \tag{28}$$

$$\mathbf{Z}_{\text{TE-TM}}^{(\delta,\gamma)} = jk\eta\{\mathbf{Q}_{11'}^{(\delta)}\}^T\,\mathbf{R}_{11}^{-1}\mathbf{E}_{12'}^{(\gamma)} + jk^3\eta \sum_{i=1}^{Q_1} \frac{\mathbf{y}_i'^{(\delta)}\{\mathbf{y}_i''^{(\gamma)}\}^T}{k_i^2(k_i^2 - k^2)} \tag{29}$$

$$\mathbf{Z}_{\text{TM-TE}}^{(\delta,\gamma)} = jk\eta\{\mathbf{E}_{12'}^{(\delta)}\}^T\,\mathbf{R}_{11}^{-1}\mathbf{Q}_{11'}^{(\gamma)} + jk^3\eta \sum_{i=1}^{Q_1} \frac{\mathbf{y}_i''^{(\delta)}\{\mathbf{y}_i'^{(\gamma)}\}^T}{k_i^2(k_i^2 - k^2)} \tag{30}$$

$$\mathbf{Z}_{\text{TM-TM}}^{(\delta,\gamma)} = \frac{\eta}{jk}\{\mathbf{Q}_{22'}^{(\delta)}\}^T\,\mathbf{S}_{22}^{-1}\mathbf{Q}_{22'}^{(\gamma)} + jk\eta\{\mathbf{E}_{12'}^{(\delta)}\}^T\,\mathbf{R}_{11}^{-1}\mathbf{E}_{12'}^{(\gamma)} + jk^3\eta \sum_{i=1}^{Q_1} \frac{\mathbf{y}_i''^{(\delta)}\{\mathbf{y}_i''^{(\gamma)}\}^T}{k_i^2(k_i^2 - k^2)} \tag{31}$$

where we have that $\mathbf{y}_i'^{(\delta)} = \{\mathbf{Q}_{11'}^{(\delta)}\}^T \mathbf{x}_i$ and $\mathbf{y}_i''^{(\delta)} = \{\mathbf{E}_{12'}^{(\delta)}\}^T \mathbf{x}_i$, $\mathbf{E}_{12'}^{(\delta)} = \mathbf{Q}_{12'}^{(\delta)} - \mathbf{S}_{12}\,\mathbf{S}_{22}^{-1}\mathbf{Q}_{22'}^{(\delta)}$, k_i and $\mathbf{x}_\mathrm{i}$ are, respectively, the eigenvalues and eigenvectors related to the inversion of the matrix **P**, the subscripts 1 and 2 refer, respectively, to TE and TM modes, and Q_1 is the number of the Q vector basis functions corresponding to TE modes.

2.1.1 Generalized *Z* matrix formulation for H-plane waveguide steps

In the previous section we derived the general formulation for any planar junction. The objective of this section is to detail the Z matrix for the H-plane waveguide junction shown in Fig. 2.

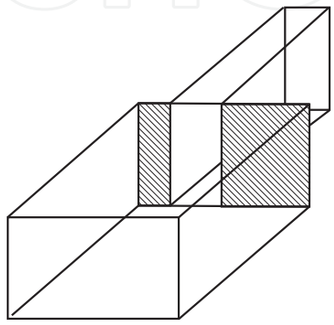

Fig. 2. H-plane junction between two waveguides.

Taking into account that only TE modes are excited in our case (H-plane junction), and considering an adequate high number of accessible modes ($N^{(\zeta)}$) in (4), such integral equation could be simplified by neglecting the second term of the kernel, thus giving place to the classical formulation collected in (Guglielmi et al., 1994). However, in order to reduce the number of accessible modes needed to get very accurate results, and therefore increasing the computational efficiency of our analysis method, we will not reject any term in the kernel of (4).

Now, with the aim of avoiding the inversion of frequency dependent matrices, the previous integral equation should be expressed in the following way

$$\mathbf{h}_n^{(\gamma)}(s) = \frac{1}{jk\eta}\int_{S^{(2)}} \mathbf{K}(s,s') \cdot \mathbf{M}_n^{(\gamma)}(s')\,ds' \tag{32}$$

being **K** a static (frequency independent) kernel. Recalling (1), it is easily verified that the first summation of (4) can be directly written as required. Regarding the second summation in (4), we can approximate the term within parenthesis by its Taylor series

$$\left(1 - \frac{Y_m^{(\zeta)}}{\hat{Y}_m^{(\zeta)}}\right) \approx \sum_{r=1}^{R} c_r \left(\frac{k_0}{\kappa_m^{(\zeta)}}\right)^{2r} \tag{33}$$

where the original frequency dependence k has been substituted by k_0 (see (7)), and c_r are the coefficients of the cited Taylor expansion for TE modes (see Table 1). As it has been explained before, if a rather high number of accessible modes is chosen for modeling the junction, we can approximate the Taylor series in (33) by zero, and then obtain the same integral equation provided by the more classical formulation (Guglielmi et al., 1994).

Thus, after introducing (1) and (33) into (4), we derive the following expression for the aforementioned static kernel

$$\mathbf{K}(s,s') = \sum_{\zeta=1}^{2}\sum_{m=1}^{\infty}\kappa_m^{(\zeta)}\mathbf{h}_m^{(\zeta)}(s)\mathbf{h}_m^{(\zeta)}(s') - \sum_{\zeta=1}^{2}\sum_{m=N^{(\zeta)}+1}^{\infty}\mathbf{h}_m^{(\zeta)}(s)\mathbf{h}_m^{(\zeta)}(s')\sum_{r=1}^{R}\frac{c_r k_0^{2r}}{\left(\kappa_m^{(\zeta)}\right)^{2r-1}} \tag{34}$$

Next, we can apply the Method of Moments to solve the integral equation proposed in (32) in the same way that for the general case, thus obtaining the next linear system of equations

$$\mathbf{P}\cdot\boldsymbol{\alpha}^{(\gamma)} = jk\eta\mathbf{Q}^{(\gamma)} \tag{35}$$

where

$$P_{p,q} = \sum_{m=1}^{\infty}\kappa_m^{(1)}\sigma_{m,p}\,\sigma_{m,q}\left[1 - F_m^{(1)}\sum_{r=1}^{R}c_r\left(\frac{k_0}{\kappa_m^{(1)}}\right)^{2r}\right] + \delta_{p,q}\kappa_p^{(2)}\left[1 - F_p^{(2)}\sum_{r=1}^{R}c_r\left(\frac{k_0}{\kappa_m^{(2)}}\right)^{2r}\right] \tag{36}$$

and $Q_{p,n}^{(\gamma)}$ has the same expression shown in (11).

Then, the matrix **P** can be inverted outside the frequency loop, thus obtaining an expression for the generalized Z matrix with a linear frequency dependence

$$\mathbf{Z}^{(\delta,\gamma)} = jk\eta\{\mathbf{Q}^{(\delta)}\}^{\mathrm{T}}\,\mathbf{P}^{-1}\mathbf{Q}^{(\gamma)} \tag{37}$$

2.2 Generalized *Y* matrix formulation

In order to derive the expressions for the elements of the generalized Y matrix of the planar waveguide junction (see Fig. 1), the next integral equation set up for the electric field at the junction plane must be solved (Gerini et al., 1998)

$$\mathbf{e}_n^{(\gamma)}(s) = \int_{S^{(\zeta)}}\sum_{\zeta=1}^{2}\left[\sum_{m=1}^{\infty}\hat{Z}_m^{(\zeta)}\mathbf{e}_m^{(\zeta)}(s)\mathbf{e}_m^{(\zeta)}(s') - \sum_{m=N^{(\zeta)}+1}^{\infty}\hat{Z}_m^{(\zeta)}\left(1-\frac{Z_m^{(\zeta)}}{\hat{Z}_m^{(\zeta)}}\right)\mathbf{e}_m^{(\zeta)}(s)\mathbf{e}_m^{(\zeta)}(s')\right]\cdot\mathbf{J}_n^{(\gamma)}(s')ds' \tag{38}$$

where $\mathbf{e}_n^{(\gamma)}$ is the electric field related to the n-th mode at waveguide γ, whereas $\mathbf{J}_n^{(\gamma)}$ is the unknown electric current at the junction plane related to the magnetic field

$$-(\mathbf{z}\times\mathbf{H}) = \sum_{n=1}^{N^{(1)}}\bar{V}_n^{(1)}\mathbf{J}_n^{(1)} - \sum_{n=1}^{N^{(2)}}\bar{V}_n^{(2)}\mathbf{J}_n^{(2)} \tag{39}$$

In order to obtain a suitable expression for the pole expansion, we can approximate the term within parenthesis in (38) by its Taylor series (see Table 1)

$$\left(1-\frac{Z_m^{(\zeta)}}{\hat{Z}_m^{(\zeta)}}\right) \approx \sum_{r=1}^{R}c_r\left(\frac{k}{\kappa_m^{(\zeta)}}\right)^{2r} \tag{40}$$

Taking into account (2), the term within parenthesis in (38) must be frequency independent for TE modes and k^2 for TM modes, so we rewrite (40) by using the wavenumber at the center of the frequency band as follows

$$\left(1-\frac{Z_m^{(\zeta)}}{\hat{Z}_m^{(\zeta)}}\right)\approx\begin{cases}\displaystyle\sum_{r=1}^{R}c_r\left(\frac{k_0}{\kappa_m^{(\zeta)}}\right)^{2r} & \text{TE}\\ \displaystyle\left(\frac{k}{k_0}\right)^2\sum_{r=1}^{R}c_r\left(\frac{k_0}{\kappa_m^{(\zeta)}}\right)^{2r} & \text{TM}\end{cases} \tag{41}$$

Now, by introducing (2) and (41) in (38), we obtain

$$\begin{aligned}\mathbf{e}_n^{(\gamma)}(s)=\sum_{\zeta=1}^{2}\int_{S^{(\zeta)}}\mathbf{J}_n^{(\gamma)}(s')\cdot\Bigg[&jk\eta\sum_{m^{\mathrm{TE}}=1}^{\infty}\frac{\mathbf{e}_m^{(\zeta)}(s)\mathbf{e}_m^{(\zeta)}(s')}{\kappa_m^{(\zeta)}}+\frac{\eta}{jk}\sum_{m^{\mathrm{TM}}=1}^{\infty}\kappa_m^{(\zeta)}\mathbf{e}_m^{(\zeta)}(s)\mathbf{e}_m^{(\zeta)}(s')\\&-jk\eta\sum_{m^{\mathrm{TE}}=N^{(\zeta)}+1}^{\infty}\mathbf{e}_m^{(\zeta)}(s)\mathbf{e}_m^{(\zeta)}(s')\sum_{r=1}^{R}\frac{c_r k_0^{2r}}{\left(\kappa_m^{(\zeta)}\right)^{2r+1}}+jk\eta\sum_{m^{\mathrm{TM}}=N^{(\zeta)}+1}^{\infty}\mathbf{e}_m^{(\zeta)}(s)\mathbf{e}_m^{(\zeta)}(s')\sum_{r=1}^{R}\frac{c_r k_0^{2r-2}}{\left(\kappa_m^{(\zeta)}\right)^{2r-1}}\Bigg]ds'\end{aligned} \tag{42}$$

The previous integral equation can be solved by means of the Method of Moments. In this case, expanding the unknown electric current in terms of the modes of the waveguide with a bigger cross-section

$$\mathbf{J}_n^{(\gamma)}(s')=\sum_{q=1}^{Q}\alpha_{q,n}^{(\gamma)}\,\mathbf{e}_q^{(1)}(s') \tag{43}$$

and using the Galerkin approach, we finally obtain the following linear system of equations in the form of (10) where

$$Q_{p,n}^{(\gamma)}=\int_{S^{(\gamma)}}\mathbf{e}_p^{(1)}(s)\,\mathbf{e}_n^{(\gamma)}(s)\,ds=\begin{cases}\delta_{p,n} & (\delta)=(1)\\ \sigma_{p,n} & (\delta)=(2)\end{cases} \tag{44}$$

$$\mathbf{P}=\frac{\eta}{jk}\left(\mathbf{R}-k^2\mathbf{S}\right) \tag{45}$$

$$R_{p,q}=\kappa_p^{(1)}\delta_{p,q}^{\mathrm{TM}}+\sum_{m^{\mathrm{TM}}=1}^{\infty}\kappa_m^{(2)}\sigma_{p,m}\,\sigma_{q,m} \tag{46}$$

$$\begin{aligned}S_{p,q}=&\frac{\delta_{p,q}^{\mathrm{TE}}}{\kappa_p^{(1)}}+\sum_{m^{\mathrm{TE}}=1}^{\infty}\frac{\sigma_{p,m}\sigma_{q,m}}{\kappa_m^{(2)}}+F_p\left(\delta_{p,q}^{\mathrm{TM}}-\left(\frac{k_0}{\kappa_p^{(1)}}\right)^2\delta_{p,q}^{\mathrm{TE}}\right)\sum_{r=1}^{R}\frac{c_r k_0^{2r-2}}{\left(\kappa_p^{(1)}\right)^{2r-1}}\\&-\sum_{m^{\mathrm{TE}}=N^{(2)}+1}^{\infty}\sigma_{p,m}\sigma_{q,m}\sum_{r=1}^{R}\frac{c_r k_0^{2r}}{\left(\kappa_m^{(2)}\right)^{2r+1}}+\sum_{m^{\mathrm{TM}}=N^{(2)}+1}^{\infty}\sigma_{p,m}\sigma_{q,m}\sum_{r=1}^{R}\frac{c_r k_0^{2r-2}}{\left(\kappa_m^{(2)}\right)^{2r-1}}\end{aligned} \tag{47}$$

Now, we express **R** and **S** as the following block matrices

$$\mathbf{R}=\begin{bmatrix}\mathbf{0}_{11} & \mathbf{0}_{12}\\ \mathbf{0}_{21} & \mathbf{R}_{22}\end{bmatrix}\qquad\mathbf{S}=\begin{bmatrix}\mathbf{S}_{11} & \mathbf{S}_{12}\\ \mathbf{S}_{21} & \mathbf{S}_{22}\end{bmatrix} \tag{48}$$

where the elements $R_{p,q}$ are zero whenever p or q are related to TE modes, since the coupling coefficients $\sigma_{p,m}$ are zero when p is a TE mode and m is a TM mode (Guillot et al., 1993). Therefore, the matrix **P** can be written as

$$\mathbf{P}=\frac{\eta}{jk}\begin{bmatrix}-k^2\mathbf{S}_{11} & -k^2\mathbf{S}_{12}\\ -k^2\mathbf{S}_{12}^{\mathrm{T}} & \mathbf{R}_{22}-k^2\mathbf{S}_{22}\end{bmatrix} \tag{49}$$

Following the same procedure that for the Z matrix computation, we obtain the inverse of the matrix $\mathbf{P}$ in the form of pole expansion

$$(\mathbf{P}^{-1})_{11}=\frac{1}{jk\eta}\mathbf{S}_{11}^{-1}+\frac{jk}{\eta}\mathbf{S}_{11}^{-1}\mathbf{S}_{12}\mathbf{R}_{22}^{-1}\mathbf{S}_{12}^{\mathrm{T}}\mathbf{S}_{11}^{-1}+\frac{jk^3}{\eta}\sum_{i=1}^{Q_2}\frac{\mathbf{x}_i'\{\mathbf{x}_i'\}^{\mathrm{T}}}{k_i^2(k_i^2-k^2)} \tag{50}$$

$$(\mathbf{P}^{-1})_{12}=-\frac{jk}{\eta}\mathbf{S}_{11}^{-1}\mathbf{S}_{12}\mathbf{R}_{22}^{-1}-\frac{jk^3}{\eta}\sum_{i=1}^{Q_2}\frac{\mathbf{x}_i'\{\mathbf{x}_i\}^{\mathrm{T}}}{k_i^2(k_i^2-k^2)} \tag{51}$$

$$(\mathbf{P}^{-1})_{22}=\frac{jk}{\eta}\mathbf{R}_{22}^{-1}+\frac{jk^3}{\eta}\sum_{i=1}^{Q_2}\frac{\mathbf{x}_i\{\mathbf{x}_i\}^{\mathrm{T}}}{k_i^2(k_i^2-k^2)} \tag{52}$$

where $\mathbf{x}_i'=\mathbf{S}_{11}^{-1}\mathbf{S}_{12}\mathbf{x}_i$. Once the $\mathbf{P}$ matrix has been successfully inverted, the elements of the Y matrix of the planar step can be obtained through the evaluation of

$$Y_{m,n}^{(\delta,\gamma)}=\sum_{q=1}^{Q}\alpha_{q,n}^{(\gamma)}\int_{S^{(\gamma)}}\mathbf{e}_q^{(1)}\,\mathbf{e}_m^{(\delta)}\,ds=\{\mathbf{Q}^{(\delta)}\}^{\mathrm{T}}\,\mathbf{P}^{-1}\mathbf{Q}^{(\gamma)} \tag{53}$$

thus obtaining the following final expressions for all possible combinations of TE and TM modes

$$\mathbf{Y}_{\text{TE-TE}}^{(\delta,\gamma)}=\frac{1}{jk\eta}\{\mathbf{Q}_{11'}^{(\delta)}\}^{\mathrm{T}}\,\mathbf{S}_{11}^{-1}\mathbf{Q}_{11'}^{(\gamma)}+\frac{jk}{\eta}\{\mathbf{E}_{21'}^{(\delta)}\}^{\mathrm{T}}\,\mathbf{R}_{22}^{-1}\mathbf{E}_{21'}^{(\gamma)}+\frac{jk^3}{\eta}\sum_{i=1}^{Q_2}\frac{\mathbf{y}_i''^{(\delta)}\{\mathbf{y}_i''^{(\gamma)}\}^{\mathrm{T}}}{k_i^2(k_i^2-k^2)} \tag{54}$$

$$\mathbf{Y}_{\text{TE-TM}}^{(\delta,\gamma)}=\frac{jk}{\eta}\{\mathbf{E}_{21'}^{(\delta)}\}^{\mathrm{T}}\,\mathbf{R}_{22}^{-1}\mathbf{Q}_{22'}^{(\gamma)}+\frac{jk^3}{\eta}\eta\sum_{i=1}^{Q_2}\frac{\mathbf{y}_i''^{(\delta)}\{\mathbf{y}_i'^{(\gamma)}\}^{\mathrm{T}}}{k_i^2(k_i^2-k^2)} \tag{55}$$

$$\mathbf{Y}_{\text{TM-TE}}^{(\delta,\gamma)}=\frac{jk}{\eta}\{\mathbf{Q}_{22'}^{(\delta)}\}^{\mathrm{T}}\,\mathbf{R}_{22}^{-1}\mathbf{E}_{21'}^{(\gamma)}+\frac{jk^3}{\eta}\eta\sum_{i=1}^{Q_2}\frac{\mathbf{y}_i'^{(\delta)}\{\mathbf{y}_i''^{(\gamma)}\}^{\mathrm{T}}}{k_i^2(k_i^2-k^2)} \tag{56}$$

$$\mathbf{Y}_{\text{TM-TM}}^{(\delta,\gamma)}=\frac{jk}{\eta}\{\mathbf{Q}_{22'}^{(\delta)}\}^{\mathrm{T}}\,\mathbf{R}_{22}^{-1}\mathbf{Q}_{22'}^{(\gamma)}+\frac{jk^3}{\eta}\eta\sum_{i=1}^{Q_2}\frac{\mathbf{y}_i'^{(\delta)}\{\mathbf{y}_i'^{(\gamma)}\}^{\mathrm{T}}}{k_i^2(k_i^2-k^2)} \tag{57}$$

where we have that $\mathbf{y}_i'^{(\delta)}=\{\mathbf{Q}_{22'}^{(\delta)}\}^{\mathrm{T}}\mathbf{x}_i$ and $\mathbf{y}_i''^{(\delta)}=\{\mathbf{E}_{21'}^{(\delta)}\}^{\mathrm{T}}\mathbf{x}_i$, $\mathbf{E}_{21'}^{(\delta)}=\mathbf{Q}_{21'}^{(\delta)}-\mathbf{S}_{12}^{\mathrm{T}}\,\mathbf{S}_{11}^{-1}\mathbf{Q}_{11'}^{(\delta)}$. As it has been explained before, the series in (54)-(57) also converge with a number of terms rather smaller than Q_2.

3. Segmentation Scheme for Passive Components based on Planar Waveguide Junctions

The structure under study is composed of the cascade connection of planar junctions between two different waveguides of lengths l_1 and l_2 (see Fig. 3), with the equivalent circuit for a Z matrix representation. Our aim is to represent each basic building block of this equivalent circuit in terms of a wideband Z matrix in the form of pole expansions

$$\mathbf{Z} = \frac{\eta}{jk}\mathbf{A} + jk\eta\mathbf{B} + jk^3\eta\mathbf{C}(\boldsymbol{\Delta}^2 - k^2\mathbf{U})^{-1}\mathbf{C}^{\mathrm{T}} \tag{58}$$

where $k = \omega\sqrt{\mu\varepsilon}$, $\eta = \sqrt{\mu/\varepsilon}$, and **A**, **B**, **C**, **Δ** and **U** are frequency independent matrices (the meaning and structure of these matrices are detailed in (Arcioni & Conciauro, 1999) for the dual case of the wideband admittance matrix formulation). In particular, **A** and **B** are square symmetric matrices of size N (N being the total number of accessible modes considered in each building block), **C** is a matrix of size $N \times Q$, with Q the number of terms included in the pole expansion, **Δ** is a diagonal matrix with the values of the poles, and **U** is the identity matrix of size Q.

According to Fig. 3, we will compute the wideband impedance matrix in the form of pole expansions for the uniform waveguide sections ($\mathbf{Z}_{w1}$ and $\mathbf{Z}_{w2}$), for each planar junction ($\mathbf{Z}_{st}$), and also for the two sets of asymptotic modal admittances generated by the integral equation technique, which are denoted as $\mathbf{Z}_{a1}$ and $\mathbf{Z}_{a2}$, respectively.

Although this method can be applied to building blocks in the form of Y matrix, in this chapter we will focus our attention in the Z matrix representation, whereas the Y matrix representation of uniform waveguides and the efficient cascade connection of Y matrices can be found in (Arcioni & Conciauro, 1999). Next, we concentrate on the novel aspects related to the efficient computation of all such matrices.

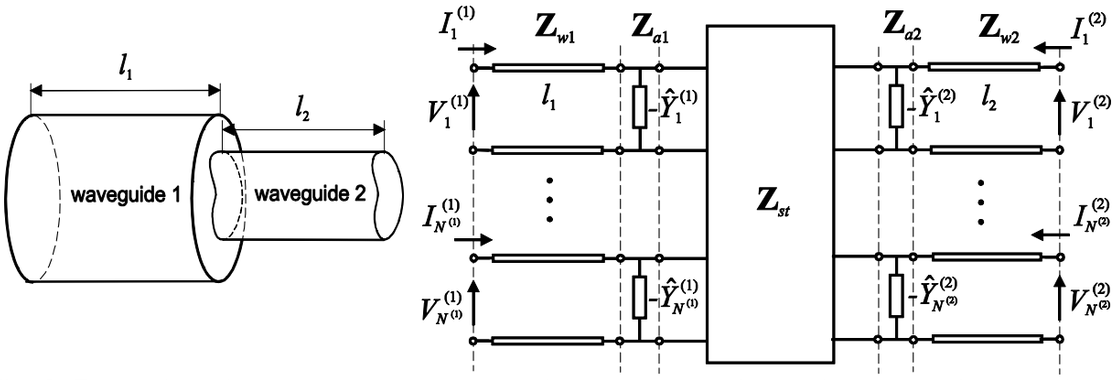

Fig. 3. Planar junction between two waveguides of lengths l_1 and l_2, and equivalent circuit for the multimode Z matrix representation.

3.1 Planar waveguide steps

If we recall the expression for the generalized impedance matrix in the form of a pole expansion (28)-(31), we find the following frequency independent blocks for the planar waveguide junction under study ($\mathbf{Z}_{st}$)

$$\mathbf{A}^{(\delta,\gamma)} = \begin{bmatrix} \mathbf{0}_{11} & \mathbf{0}_{12} \\ \mathbf{0}_{21} & \{\mathbf{Q}_{22}^{(\delta)}\}^{\mathrm{T}}\mathbf{S}_{22}^{-1}\mathbf{Q}_{22}^{(\gamma)} \end{bmatrix} \tag{59}$$

$$\mathbf{B}^{(\delta,\gamma)} = \begin{bmatrix} \{\mathbf{Q}_{11}^{(\delta)}\}^{\mathrm{T}}\mathbf{R}_{11}^{-1}\mathbf{Q}_{11}^{(\gamma)} & \{\mathbf{Q}_{11}^{(\delta)}\}^{\mathrm{T}}\mathbf{R}_{11}^{-1}\mathbf{E}_{12}^{(\gamma)} \\ \{\mathbf{E}_{12}^{(\delta)}\}^{\mathrm{T}}\mathbf{R}_{11}^{-1}\mathbf{Q}_{11}^{(\gamma)} & \{\mathbf{E}_{12}^{(\delta)}\}^{\mathrm{T}}\mathbf{R}_{11}^{-1}\mathbf{E}_{12}^{(\gamma)} \end{bmatrix} \tag{60}$$

$$\mathbf{C} = \begin{bmatrix} \mathbf{Y}'^{(1)}\Delta^{-1} \\ \mathbf{Y}''^{(1)}\Delta^{-1} \\ \mathbf{Y}'^{(2)}\Delta^{-1} \\ \mathbf{Y}''^{(2)}\Delta^{-1} \end{bmatrix} \quad \boldsymbol{\Delta} = \mathrm{diag}\{k_1, \ldots, k_{Q_1}\} \tag{61}$$

where $\mathbf{Y}'^{(\delta)} = [\mathbf{y}_1'^{(\delta)} \ldots \mathbf{y}_{Q_1}'^{(\delta)}]$ and $\mathbf{Y}''^{(\delta)} = [\mathbf{y}_1''^{(\delta)} \ldots \mathbf{y}_{Q_1}''^{(\delta)}]$ for $\delta = 1,2$.

3.2 Asymptotic admittances

Each set of asymptotic modal admittances in Fig. 3 can be seen as a two-port network, which can be easily characterized by a generalized Z matrix ($\mathbf{Z}_a$) whose elements are defined as follows

$$Z_{m,n}^{(\delta,\gamma)} = -\frac{\delta_{mn}}{\hat{Y}_m} = \delta_{mn} \begin{cases} -\dfrac{jk\eta}{\kappa_m^{(\delta)}} & \text{TE} \\ -\dfrac{\kappa_m^{(\delta)}\eta}{jk} & \text{TM} \end{cases} \tag{62}$$

The previous expression is suitable for the representation of the generalized impedance matrix as indicated by (58). In this case, the pole expansion is not present and therefore

$$A_{mn}^{(\delta,\gamma)} = \delta_{mn} \begin{cases} 0 & \text{TE} \\ -\kappa_m^{(\delta)} & \text{TM} \end{cases} \tag{63}$$

$$B_{mn}^{(\delta,\gamma)} = \delta_{mn} \begin{cases} -1/\kappa_m^{(\delta)} & \text{TE} \\ 0 & \text{TM} \end{cases} \tag{64}$$

3.3 Uniform waveguide sections

Now, we derive the expressions for the generalized impedance matrix of a uniform waveguide section of length l. Since the modes of this element are uncoupled, the only non-zero entries of such Z matrix ($\mathbf{Z}_w$) are those relating voltages and currents of the same mode, which are computed as

$$Z_{mn}^{(1,1)} = Z_{mn}^{(2,2)} = \delta_{mn} Z_m \coth \gamma_m l \tag{65}$$

$$Z_{mn}^{(1,2)} = Z_{mn}^{(2,1)} = \delta_{mn} Z_m \mathrm{csch}\, \gamma_m l \tag{66}$$

where $\gamma_m = \sqrt{\kappa_m^2 - k^2}$, and κ_m and Z_m are, respectively, the cutoff wavenumber and the characteristic impedance of the m-th mode considered in the waveguide section.

Considering that the modes of the waveguide section can be of type TE or TM, we obtain the following expressions

$$Z_{mn}^{(1,1)} = \delta_{mn} \begin{cases} jk\eta \dfrac{\coth \gamma_m l}{\gamma_m} = jk\eta f_r^{\mathrm{TE}}(k^2) & \text{TE} \\ \dfrac{\eta}{jk}\gamma_m \coth \gamma_m l = \dfrac{\eta}{jk} f_r^{\mathrm{TM}}(k^2) & \text{TM} \end{cases} \tag{67}$$

$$Z_{mn}^{(1,2)} = \delta_{mn} \begin{cases} jk\eta \dfrac{\operatorname{csch}\kappa_m l}{\gamma_m} = jk\eta f_t^{\mathrm{TE}}(k^2) & \text{TE} \\ \dfrac{\eta}{jk}\gamma_m \operatorname{csch}\kappa_m l = \dfrac{\eta}{jk} f_t^{\mathrm{TM}}(k^2) & \text{TM} \end{cases} \tag{68}$$

In order to express the Z matrix elements of the waveguide section in the form of the pole expansion collected in (58), we will make use of the theorem of Mittag-Leffler (Spiegel, 1991)

$$f(k^2) = f(0) + \sum_{p=1}^{\infty} \operatorname{Re}s(f, z_p) \frac{k^2}{z_p(k^2 - z_p)} \tag{69}$$

where $\operatorname{Re}s(f, z_p)$ are the residues of the function f related to their poles z_p, which in our case are defined as

$$z_p \equiv k_{ms}^2 = (\kappa_m^{(1)})^2 + (s\pi / l)^2 \tag{70}$$

with $s = 0,1,2,\ldots$ for TE modes and $s = 1,2,3,\ldots$ for TM modes. It can be seen that the values for the poles are directly related to the resonant wavenumbers of the open-circuited waveguide.

Then, applying the theorem of Mittag-Leffler to the functions f in equations (67) and (68), we can obtain

$$f_r^{\mathrm{TE}}(k^2) = \frac{\coth\kappa_m l}{\kappa_m} + k^2 \sum_{s=0}^{\infty} \frac{\varepsilon_s}{l} \frac{1}{k_{ms}^2(k_{ms}^2 - k^2)} \tag{71}$$

$$f_r^{\mathrm{TM}}(k^2) = \kappa_m \coth\kappa_m l - k^2 \frac{2}{l} \sum_{s=1}^{\infty} \frac{(s\pi / l)^2}{k_{ms}^2(k_{ms}^2 - k^2)} \tag{72}$$

$$f_t^{\mathrm{TE}}(k^2) = \frac{\operatorname{csch}\kappa_m l}{\kappa_m} + k^2 \sum_{s=0}^{\infty} \frac{\varepsilon_s}{l} \frac{(-1)^s}{k_{ms}^2(k_{ms}^2 - k^2)} \tag{73}$$

$$f_t^{\mathrm{TM}}(k^2) = \kappa_m \operatorname{csch}\kappa_m l - k^2 \frac{2}{l} \sum_{s=1}^{\infty} \frac{(-1)^s (s\pi / l)^2}{k_{ms}^2(k_{ms}^2 - k^2)} \tag{74}$$

where ε_s means the Neumann's factor (i.e. $\varepsilon_s = 1$ if $s = 0$ and $\varepsilon_s = 2$ if $s \neq 0$).

For the case of the f_r^{TM} and f_t^{TM} functions we need further treatment of the previous expressions. In particular, we must extract the low frequency contribution from the series in (72) and (74). Then, after solving analytically the infinite summations when $k \to 0$ (Gradstheyn and Ryzhik, 1980), we can obtain that

$$f_r^{\mathrm{TM}}(k^2) = \kappa_m \coth\kappa_m l - k^2 \frac{l}{2}\left(\frac{\coth\kappa_m l}{\kappa_m l} - \operatorname{csch}^2\kappa_m l\right) - k^4 \frac{2}{l} \sum_{s=1}^{\infty} \frac{(s\pi / l)^2}{k_{ms}^4(k_{ms}^2 - k^2)} \tag{75}$$

$$f_t^{\mathrm{TM}}(k^2) = \kappa_m \operatorname{csch}\kappa_m l - k^2 \frac{l}{2} \operatorname{csch}\kappa_m l \left(\frac{1}{\kappa_m l} - \coth\kappa_m^{(1)} l\right) - k^4 \frac{2}{l} \sum_{s=1}^{\infty} \frac{(-1)^s (s\pi / l)^2}{k_{ms}^4(k_{ms}^2 - k^2)} \tag{76}$$

Finally, if we introduce the previous expansions (71), (73), (75) and (76) into (67) and (68), we obtain the Z matrix representation in the form of (58), where the entries of the frequency independent matrices are

$$A_{m,n}^{(1,1)} = \delta_{mn} \begin{cases} 0 & \text{TE} \\ \kappa_m \coth \kappa_m l & \text{TM} \end{cases} \qquad A_{m,n}^{(1,2)} = \delta_{mn} \begin{cases} 0 & \text{TE} \\ \kappa_m \operatorname{csch} \kappa_m l & \text{TM} \end{cases} \tag{77}$$

$$B_{m,n}^{(1,1)} = \delta_{mn} \begin{cases} \dfrac{\coth \kappa_m l}{\kappa_m} & \text{TE} \\ \dfrac{1}{2}\left(\dfrac{\coth \kappa_m l}{\kappa_m l} - \operatorname{csch}^2 \kappa_m l \right) & \text{TM} \end{cases} \qquad B_{m,n}^{(1,2)} = \delta_{mn} \begin{cases} \dfrac{\operatorname{csch} \kappa_m l}{\kappa_m} & \text{TE} \\ \dfrac{1}{2} \operatorname{csch}^2 \kappa_m l \left(\dfrac{1}{\kappa_m l} - \coth \kappa_m l \right) & \text{TM} \end{cases} \tag{78}$$

$$\mathbf{C} = \begin{bmatrix} \mathbf{C}^{(1)} \\ \mathbf{C}^{(2)} \end{bmatrix} \qquad C_{m,ns}^{(1)} = \delta_{mn} \begin{cases} \sqrt{\dfrac{\varepsilon_s}{l}} \dfrac{1}{k_{ms}} & \text{TE} \\ \sqrt{\dfrac{2}{l}} \dfrac{(s\pi / l)}{k_{ms}^2} & \text{TM} \end{cases} \qquad C_{m,ns}^{(2)} = (-1)^s C_{m,ns}^{(1)} \tag{79}$$

4. Efficient Cascade Connection of *Z* Matrices

Once the expressions for the generalized Z matrices of all basic blocks of the structure shown in Fig. 3 have been presented, we proceed to combine them in order to determine the wideband Z matrix representation of the complete structure. For such purpose, we first outline a procedure to solve the combination of two cascaded Z matrices in the form of pole expansions, which follows a dual formulation to the one derived in (Arcioni & Conciauro, 1999) for the admittance matrix case. Then, a novel efficient algorithm, which allows to reduce the effective number of poles to be considered after connecting two wideband Z matrices, is fully described.

4.1 Combination of two generalized *Z* matrices

Let us consider two cascaded building blocks of the structure shown in Fig. 3, whose generalized Z matrices (named as $\mathbf{Z}_I$ and $\mathbf{Z}_{II}$ in Fig. 4) are given in the previous form of (58). As it can be inferred from Fig. 4, the voltages and the currents at the external ports are grouped into the vectors $\mathbf{v}^{(1)}$, $\mathbf{i}^{(1)}$, $\mathbf{v}^{(2)}$ and $\mathbf{i}^{(2)}$, and the currents at the connected ports are collected into the vector $\mathbf{i}^{(c)}$. If we consider that the currents $\mathbf{i}^{(1)}$ and $\mathbf{i}^{(2)}$ are incoming, respectively, to the blocks I and II, and the currents $\mathbf{i}^{(c)}$ are incoming to the block II, we can write

$$\mathbf{v} = \mathbf{Z}^{ee}\, \mathbf{i} + \mathbf{Z}^{ec}\, \mathbf{i}^{(c)} \tag{80}$$

$$\mathbf{Z}^{cc}\, \mathbf{i}^{(c)} = -\{\mathbf{Z}^{ec}\}^{\mathrm{T}}\, \mathbf{i} \tag{81}$$

where

$$\mathbf{v} = \begin{bmatrix} \mathbf{v}^{(1)} \\ \mathbf{v}^{(2)} \end{bmatrix} \qquad \mathbf{i} = \begin{bmatrix} \mathbf{i}^{(1)} \\ \mathbf{i}^{(2)} \end{bmatrix} \tag{82}$$

and the matrices $\mathbf{Z}^{ee}$, $\mathbf{Z}^{ec}$ and $\mathbf{Z}^{cc}$ are given by

$$\mathbf{Z}^{ee} = \begin{bmatrix} \mathbf{Z}_I^{(1,1)} & 0 \\ 0 & \mathbf{Z}_{II}^{(2,2)} \end{bmatrix} \quad \mathbf{Z}^{ec} = \begin{bmatrix} -\mathbf{Z}_I^{(1,c)} \\ \mathbf{Z}_{II}^{(2,c)} \end{bmatrix} \quad \mathbf{Z}^{cc} = \mathbf{Z}_I^{(c,c)} + \mathbf{Z}_{II}^{(c,c)} \tag{83}$$

Our final goal is to obtain the overall matrix $\mathbf{Z}_{tot}$, relating the vectors $\mathbf{v}$ and $\mathbf{i}$, in the same form of (58). For such purpose, we first express the matrices $\mathbf{Z}^{ee}$, $\mathbf{Z}^{ec}$ and $\mathbf{Z}^{cc}$ in the form of pole expansions. Taking into account the following definitions of the matrices

$$\mathbf{A}^{ee} = \begin{bmatrix} \mathbf{A}_I^{(1,1)} & 0 \\ 0 & \mathbf{A}_{II}^{(2,2)} \end{bmatrix} \qquad \mathbf{B}^{ee} = \begin{bmatrix} \mathbf{B}_I^{(1,1)} & 0 \\ 0 & \mathbf{B}_{II}^{(2,2)} \end{bmatrix} \qquad \mathbf{C}^{ee} = \begin{bmatrix} \mathbf{C}_I^{(1)} & 0 \\ 0 & \mathbf{C}_{II}^{(2)} \end{bmatrix} \tag{84}$$

$$\mathbf{A}^{cc} = \begin{bmatrix} \mathbf{A}_I^{(c,c)} + \mathbf{A}_{II}^{(c,c)} \end{bmatrix} \qquad \mathbf{B}^{cc} = \begin{bmatrix} \mathbf{B}_I^{(c,c)} + \mathbf{B}_{II}^{(c,c)} \end{bmatrix} \qquad \mathbf{C}^{c} = \begin{bmatrix} -\mathbf{C}_I^{(c)} & \mathbf{C}_{II}^{(c)} \end{bmatrix} \tag{85}$$

$$\mathbf{A}^{ec} = \begin{bmatrix} -\mathbf{A}_I^{(1,c)} \\ \mathbf{A}_{II}^{(2,c)} \end{bmatrix} \qquad \mathbf{B}^{ec} = \begin{bmatrix} -\mathbf{B}_I^{(1,c)} \\ \mathbf{B}_{II}^{(2,c)} \end{bmatrix} \qquad \mathbf{\Delta} = \begin{bmatrix} \mathbf{\Delta}_I & 0 \\ 0 & \mathbf{\Delta}_{II} \end{bmatrix} \tag{86}$$

we can easily write that

$$\mathbf{Z}^{ee} = \frac{\eta}{jk}\mathbf{A}^{ee} + jk\eta\mathbf{B}^{ee} + jk^3\eta\mathbf{C}^{e}(\mathbf{\Delta}^2 - k^2\mathbf{U})^{-1}\{\mathbf{C}^{e}\}^{\mathrm{T}} \tag{87}$$

$$\mathbf{Z}^{ec} = \frac{\eta}{jk}\mathbf{A}^{ec} + jk\eta\mathbf{B}^{ec} + jk^3\eta\mathbf{C}^{e}(\mathbf{\Delta}^2 - k^2\mathbf{U})^{-1}\{\mathbf{C}^{c}\}^{\mathrm{T}} \tag{88}$$

$$\mathbf{Z}^{cc} = \frac{\eta}{jk}\mathbf{A}^{cc} + jk\eta\mathbf{B}^{cc} + jk^3\eta\mathbf{C}^{c}(\mathbf{\Delta}^2 - k^2\mathbf{U})^{-1}\{\mathbf{C}^{c}\}^{\mathrm{T}} \tag{89}$$

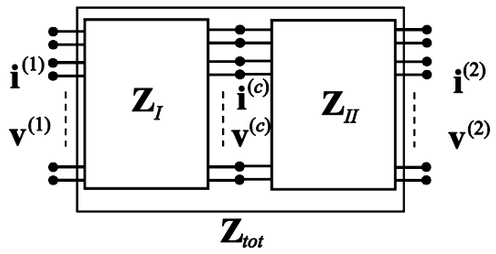

Fig. 4. Two elementary building blocks connected in cascade.

Then, the currents at the connected ports can be arranged in the following way

$$\mathbf{i}^{(c)} = \begin{bmatrix} \mathbf{i}_1^c \\ \mathbf{i}_2^c \end{bmatrix} \tag{90}$$

where $\mathbf{i}_1^c$ and $\mathbf{i}_2^c$ contain, respectively, the currents corresponding to TE (subscript 1) and TM (subscript 2) modes. According to such arrangement, the related matrices of (84)-(86) can be partitioned as indicated below

$$\mathbf{A}^{cc} = \begin{bmatrix} 0 & 0 \\ 0 & \mathbf{A}_{22}^{cc} \end{bmatrix} \qquad \mathbf{B}^{cc} = \begin{bmatrix} \mathbf{B}_{11}^{cc} & \mathbf{B}_{12}^{cc} \\ \left\{\mathbf{B}_{12}^{cc}\right\}^T & \mathbf{B}_{22}^{cc} \end{bmatrix} \qquad \mathbf{C}^{c} = \begin{bmatrix} \mathbf{C}_1^c \\ \mathbf{C}_2^c \end{bmatrix} \tag{91}$$

$$\mathbf{A}^{ec} = \begin{bmatrix} 0 & \mathbf{A}_2^{ec} \end{bmatrix} \qquad \mathbf{B}^{ec} = \begin{bmatrix} \mathbf{B}_1^{ec} & \mathbf{B}_2^{ec} \end{bmatrix} \tag{92}$$

where zero matrices appear in the partitioning of $\mathbf{A}^{cc}$ and $\mathbf{A}^{ec}$ when TE modes are involved (remember the expressions collected in (59), (63) and (77)). At this point, the problem to be solved is completely dual to the one considered in (Arcioni & Conciauro, 1999) for the admittance matrix formulation. Therefore, following a dual procedure, we can easily deduce

the Z matrix for the cascaded connection of the building blocks in the required form of pole expansions

$$\mathbf{Z}_{tot} = \frac{\eta}{jk}\mathbf{A}_{tot} + jk\eta\mathbf{B}_{tot} + jk^3\eta\mathbf{C}_{tot}(\mathbf{K}^2 - k^2\mathbf{U})^{-1}\mathbf{C}_{tot}^{\mathrm{T}} \tag{93}$$

where

$$\mathbf{A}_{tot} = \mathbf{A}^{ee} - \mathbf{A}_2^{ec}\{\mathbf{A}_{22}^{cc}\}^{-1}\{\mathbf{A}_2^{ec}\}^{\mathrm{T}} \tag{94}$$

$$\mathbf{B}_{tot} = \mathbf{E} + \mathbf{A}_2^{ec}\mathbf{X}_{\mathrm{i}}\mathbf{K}^{-4}\mathbf{X}_{\mathrm{i}}^{\mathrm{T}}\{\mathbf{A}_2^{ec}\}^{\mathrm{T}} - \mathbf{A}_2^{ec}\{\mathbf{A}_{22}^{cc}\}^{-1}\mathbf{F}^{\mathrm{T}} - \mathbf{F}\{\mathbf{A}_{22}^{cc}\}^{-1}\{\mathbf{A}_2^{ec}\}^{\mathrm{T}} \tag{95}$$

$$\mathbf{C}_{tot} = \mathbf{F}\mathbf{X}_{\mathrm{i}} + \mathbf{G}\mathbf{X}_{\mathrm{w}} - \mathbf{A}_2^{ec}\mathbf{X}_{\mathrm{i}}\mathbf{K}^{-2} \tag{96}$$

and

$$\mathbf{E} = \mathbf{B}^{ee} - \mathbf{B}_1^{ec}\{\mathbf{B}_{11}^{cc}\}^{-1}\{\mathbf{B}_1^{ec}\}^{\mathrm{T}} \tag{97}$$

$$\mathbf{F} = \mathbf{B}_2^{ec} - \mathbf{B}_1^{ec}\{\mathbf{B}_{11}^{cc}\}^{-1}\mathbf{B}_{12}^{cc} \tag{98}$$

$$\mathbf{G} = \mathbf{C}^{e} - \mathbf{B}_1^{ec}\{\mathbf{B}_{11}^{cc}\}^{-1}\mathbf{C}_1^{c} \tag{99}$$

Furthermore, the matrix $\mathbf{K} = \mathrm{diag}\{k_i\}$ is a diagonal matrix with the eigenvalues, and $\mathbf{X}_{\mathrm{i}}$ and $\mathbf{X}_{\mathrm{w}}$ are matrices with the eigenvectors, corresponding to the solution of the problem

$$\left(\begin{bmatrix}\mathbf{A}_{22}^{cc} & 0\\ 0 & \boldsymbol{\Delta}^2\end{bmatrix} - k^2\begin{bmatrix}\mathbf{P} & \mathbf{R}\\ \mathbf{R}^{\mathrm{T}} & \mathbf{Q}\end{bmatrix}\right)\begin{bmatrix}\mathbf{i}_2^{c}\\ \mathbf{w}^{c}\end{bmatrix} = 0 \tag{100}$$

where

$$\mathbf{P} = \mathbf{B}_{22}^{cc} - \{\mathbf{B}_{12}^{cc}\}^{\mathrm{T}}\{\mathbf{B}_{11}^{cc}\}^{-1}\mathbf{B}_{12}^{cc} \tag{101}$$

$$\mathbf{Q} = \mathbf{U} - \{\mathbf{C}_1^{c}\}^{\mathrm{T}}\{\mathbf{B}_{11}^{cc}\}^{-1}\mathbf{C}_1^{c} \tag{102}$$

$$\mathbf{R} = \mathbf{C}_2^{c} - \{\mathbf{B}_{12}^{cc}\}^{\mathrm{T}}\{\mathbf{B}_{11}^{cc}\}^{-1}\mathbf{C}_1^{c} \tag{103}$$

and the auxiliary vector $\mathbf{w}^c$ is defined as follows

$$\mathbf{w}^{c} = k^2\left(\boldsymbol{\Delta}^2 - k^2\mathbf{U}\right)^{-1}\left(\{\mathbf{C}^{e}\}^{\mathrm{T}}\mathbf{i} + \{\mathbf{C}_1^{c}\}^{\mathrm{T}}\mathbf{i}_1^{c} + \{\mathbf{C}_2^{c}\}^{\mathrm{T}}\mathbf{i}_2^{c}\right) \tag{104}$$

4.2 Efficient characterization of passive structures

When two building blocks of a structure are cascaded, the number of terms in the resulting pole expansion is equal to the number of poles for each block plus the number of TM accessible modes at the common port (see the generalized eigenvalue problem raised in (100), as well as the definition and partitioning of the involved matrices in (84)-(86), (91) and (92)). If the structure is composed of many blocks, the total number of poles will become very high, thus reducing the efficiency of the algorithm due to the size of the successive eigenvalue problems.

For avoiding such drawback, we propose to limit the number of eigenvalues considered after each connection. When two different blocks are connected, we obtain the entries of the generalized Z matrix in the following form

$$Z_{mn}^{(\delta,\gamma)} = \frac{\eta}{jk}A_{mn}^{(\delta,\gamma)} + jk\eta B_{mn}^{(\delta,\gamma)} + jk^3\eta\sum_{i=1}^{Q}\frac{C_{mi}^{(\delta)}C_{ni}^{(\gamma)}}{k_i^2 - k^2} \tag{105}$$

In this equation, the higher terms of the sum have a lower contribution to the final result. Due to this fact, we can only consider Q' eigenvalues in the sum, and approximate the contribution of the remaining $Q-Q'$ eigenvalues by

$$jk^3\eta \sum_{i=Q'+1}^{Q} \frac{C_{mi}^{(\delta)} C_{ni}^{(\gamma)}}{k_i^2 - k^2} \approx jkk_0^2\eta \sum_{i=Q'+1}^{Q} \frac{C_{mi}^{(\delta)} C_{ni}^{(\gamma)}}{k_i^2 - k_0^2} \tag{106}$$

where k_0 corresponds to the value of k at the center point of the frequency band. Proceeding in such a way, the eigenvalues with lower weight are included within the linear term

$$Z_{mn}^{(\delta,\gamma)} \approx \frac{\eta}{jk} A_{mn}^{(\delta,\gamma)} + jk\eta \left(B_{mn}^{(\delta,\gamma)} + k_0^2 \sum_{i=Q'+1}^{Q} \frac{C_{mi}^{(\delta)} C_{ni}^{(\gamma)}}{k_i^2 - k_0^2} \right) + jk^3\eta \sum_{i=1}^{Q'} \frac{C_{mi}^{(\delta)} C_{ni}^{(\gamma)}}{k_i^2 - k^2} \tag{107}$$

thus obtaining a reduced size for the eigenvalue problem to be solved during the next connection, whereas very good accuracy is still preserved. This technique can also be applied to reduce the number of poles involved in the Z matrix characterization of each single building block, i.e. waveguide steps and uniform waveguide sections.

5. Optimized Cascade Connection for H-plane Waveguide Components

The method proposed in the previous section is general and can be simplified for the analysis of H-plane components, where only TE modes are present. However, the absence of TM modes involves that the **A** matrices for all the building blocks are zero. For this reason, we introduce a new general expression for the building blocks where an additional low frequency term depending on k^3 has been extracted

$$\mathbf{Z} = jk\eta\mathbf{A} + jk^3\eta\mathbf{B} + jk^5\eta\mathbf{C}(\boldsymbol{\Delta}^2 - k^2\mathbf{U})^{-1}\mathbf{C}^{\mathrm{T}} \tag{108}$$

The purpose of this new formulation is to obtain new expressions of the matrix **C** with a stronger attenuation for higher terms in the pole expansion. In this way, a lower number of poles will be neccessary for recovering a given accuracy.
The proposed cascade connection in section 4.1 can be applied since (108) can be expressed in the following way

$$\mathbf{Z} = k^2 \left(\frac{\eta}{jk}(-\mathbf{A}) + jk\eta\mathbf{B} + jk^3\eta\mathbf{C}(\boldsymbol{\Delta}^2 - k^2\mathbf{U})^{-1}\mathbf{C}^{\mathrm{T}} \right) \tag{109}$$

5.1 Uniform waveguide section for H-plane waveguide components

Equations (71) and (73) provide the expression for $f_r^{\mathrm{TE}}(k^2)$ and $f_t^{\mathrm{TE}}(k^2)$ for a Z matrix expression in the form of (58). However, in order to obtain the Z matrix in the form of (108) for H-plane components, an additional low frequency term must be extracted from the series in (71) and (73). Then, after solving analytically the infinite summations when $k \to 0$ (Gradstheyn and Ryzhik, 1980), we obtain the following expressions for the functions f^{TE}

$$f_r^{TE}(k^2) = \frac{\coth \kappa_m l}{\kappa_m} + k^2 \frac{l}{2(\kappa_m)^2}\left[\frac{\coth \kappa_m l}{\kappa_m l} + \operatorname{csch}^2 \kappa_m l\right] + k^4 \sum_{s=1}^{\infty} \frac{\varepsilon_s}{l} \frac{1}{k_{ms}^4 (k_{ms}^2 - k^2)} \tag{110}$$

$$f_t^{TE}(k^2) = \frac{\operatorname{csch} \kappa_m l}{\kappa_m} + k^2 \frac{1 + \kappa_m l \coth \kappa_m l}{2\kappa_m^3 \sinh^2 \kappa_m l} + k^4 \sum_{s=1}^{\infty} \frac{\varepsilon_s}{l} \frac{(-1)^s}{k_{ms}^4 (k_{ms}^2 - k^2)} \tag{111}$$

Finally, after introducing the previous expansions (110) and (111) into (67) and (68), it can be easily identified the entries of the frequency independent blocks corresponding to the wideband *Z* matrix representation of the waveguide section

$$A_{m,n}^{(1,1)} = \delta_{mn} \frac{\coth \kappa_m l}{\kappa_m} \qquad A_{m,n}^{(1,2)} = \delta_{mn} \frac{\operatorname{csch} \kappa_m l}{\kappa_m} \tag{112}$$

$$B_{m,n}^{(1,1)} = \delta_{mn} \frac{l}{2\kappa_m^2}\left(\frac{\coth \kappa_m l}{\kappa_m l} + \operatorname{csch}^2 \kappa_m l\right) \qquad B_{m,n}^{(1,2)} = \delta_{mn} \frac{1 + \kappa_m l \coth \kappa_m l}{2\kappa_m^3 \sinh^2 \kappa_m l} \tag{113}$$

$$C_{m,ns}^{(1)} = \delta_{mn} \sqrt{\frac{\varepsilon_s}{l}} \frac{1}{k_{ms}^2} \qquad C_{m,ns}^{(2)} = (-1)^s C_{m,ns}^{(1)} \tag{114}$$

If the expression of the C entries in (114) is compared with (79), the new entries depend on $1/k_{ms}^2$ instead of $1/k_{ms}$, thus reducing the required number of poles because of the stronger attenuation of the terms in the series.

6. Validation Results

First of all, we have performed a detailed convergence study of the impedance and admittance formulations of the original integral equation technique proposed in (Gerini et al., 1998). From this study, we conclude that accurate and stable results are obtained in both cases, provided that the same number of modes in the bigger and smaller waveguides is used with each formulation, and that the higher number of modes is always chosen for the bigger waveguide. Note that in the *Z* matrix (*Y* matrix) formulation, the basis functions are the modes of the smaller (bigger) cross-section waveguide, whereas the infinite series involve the modes of the bigger (smaller) waveguide. This means that the number of basis functions in the *Y* matrix formulation should be equal to the number of terms considered in the infinite series present in the *Z* matrix representation, and vice versa. Since the classical integral equation technique needs to invert a matrix of size equal to the number of basis functions per each frequency point, the *Y* matrix formulation provides the slowest convergent results. To accelerate such convergence rate, we propose the wideband representation just outlined in this work.

For verification purposes, we have first analyzed a simple planar junction between two rectangular waveguides (see the geometry in Fig. 5). First of all, we proceed to validate the *Z* matrix formulation through comparison with the original integral equation technique. In Fig. 5 (left), we show the results obtained for 1, 8 and 15 accessible modes (*N*), whereas the total number of basis functions (*Q*) is equal to 100 (Q_1=58), *R*=3 in (7), and the infinite series in (13) and (14) are summed up with 600 terms. With regard to the convergent evaluation of the frequency-dependent series in (28)-(31), only the first 25 terms (poles) have been required. For comparative reasons, we also include the results for k_0=0 in (7), which

correspond to the ones provided by the method proposed in (Mira et al., 2006), and the convergent results obtained with the original integral equation technique using only 1 accessible mode. It can be concluded that the use of k_0 clearly improves the convergence rate of our method, thus involving a reduction in the required number of accessible modes (N) when compared to the previous approach of (Mira et al., 2006).

In terms of numerical efficiency, the CPU time required by our method to solve the considered waveguide step in the whole frequency range (201 frequency points) has been equal to 0.10 s[1] for the worst case (N=15). However, the original integral equation technique needed 1.01 s for solving the same planar junction. Therefore, the analysis method of planar waveguide junctions proposed in this paper involves a substantial reduction in the related computational effort, without degrading the accuracy of results.

In Fig. 5 (right) we compare the obtained results for Z matrix and Y matrix formulations. As it can be noticed, with an adequate number of accessible modes (i.e. N=15) the Y matrix formulation provides the same accurate results. Only small differences can be observed for 1 accesible mode, because of the different aproximations proposed in (7) and (41). In terms of numerical efficiency, the CPU time required by using the Y matrix formulation to solve the waveguide step in the whole frequency range has been equal to 0.55 s for the worst case. The original integral equation technique would need 108 s following the Y matrix formulation.

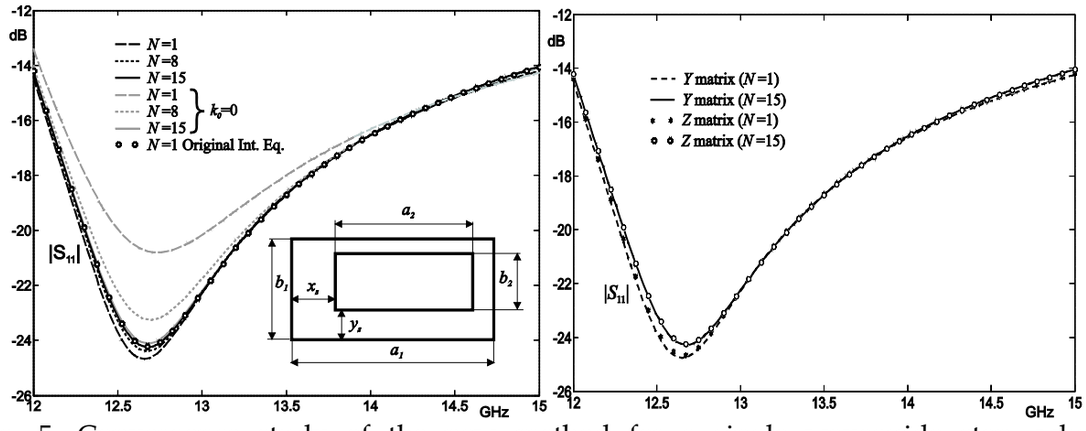

Fig. 5. Convergence study of the new method for a single waveguide step, whose dimensions are a_1=19.05 mm, b_1=9.525 mm, a_2=13.0 mm, b_2=5.5 mm, x_s=4.0 mm and y_s=3.0 mm.

Once the algorithm for the analysis of single waveguide steps has been successfully verified, the analysis of several waveguide filters will be shown for validating the overall performance of the proposed technique. Our first example deals with the full-wave analysis of a 4-pole direct-coupled cavity filter in WR-75 waveguide (a=19.05 mm, b=9.525 mm). The dimensions of the coupling windows (see Fig. 6) are w_1=9.55 mm, w_2=6.49 mm and w_3=5.89 mm, h_1=h_2=h_3=6.0 mm and d=2.0 mm, whereas the lengths of the WR-75 waveguide cavities are l_1=11.95 mm and l_2=13.37 mm. In order to get an accurate modelling of all waveguide

[1]All reported CPU times have been obtained with a Pentium 4 at 3.2 GHz.

steps involved in this example, we have considered N=9, Q=450 and 75 terms in the series (Z matrix formulation), where the symmetries of the structure have been taken into account.
The practical application of the iterative algorithm of Section 4 has been implemented in the same way for all the filter examples. First, the cascade connection of the generalized matrices representing each waveguide step, and their related two sets of asymptotic admittances (see Fig. 3), has been solved. Next, the generalized matrices representing the uniform waveguide sections have been added. Finally, all these basic building blocks are cascaded in order to obtain the overall Z matrix for the whole structure. In order to reduce the overall number of poles, the algorithm proposed in Section 4.2 has been applied after each cascade connection. In this example, the final number of poles related to the last cascade connection was equal to 60.
In Fig. 6, we successfully compare the set of S parameters obtained with our pole expansion technique (solid lines) with those provided by the well-known commercial software Ansoft HFSS (v.10.0) based on the Finite Elements Method (FEM). In order to evaluate the numerical efficiency related to the analysis technique proposed in this paper, we have also made use of a traditional approach based on frequency-by-frequency (point-to-point) calculations for solving the cascade connection of Z matrices (see for instance (Boria et al., 1997)). As it can be concluded from Fig. 6 (see results with stars), the same accurate response can be obtained with the point-to-point cascade connection technique. However, the CPU effort required by such traditional approach to compute the electrical response for 301 frequency values was equal to 0.54 s, whereas following the method proposed in this paper was reduced to only 0.23 s. If the original integral equation technique is used to analyze the planar waveguide steps, together with the point-to-point connection technique, the same accurate results from Fig. 6 can be recovered in 2.68 s, and 1490 s with HFSS (fast sweep).
Therefore, it can be concluded that our novel analysis technique is the most efficient one in terms of computational effort. Furthermore, we have verified that the CPU time required by our method remains rather stable with the required number of frequency points, thus making it very appropriate for dense simulations in the frequency domain. Finally, we have also included in Fig. 6 the results obtained when k_0=0 in (7) and (107). As it could be expected, such results converge more slowly than those provided by our analysis technique.
The analysis by means of Y matrix formulation has been also performed, but in this case only with the point-to-point connection technique. In this case the total CPU time was 1.20 s with our new formulation, and 239 s following the classical Y matrix formulation.
The second example consists of a triple-mode filter proposed in (Lastoria et al., 1998), whose topology is shown in Fig. 7. The input and output sections of this filter are standard WR-75 waveguides, and the dimensions of the five inner waveguides are a_1=12.2 mm, a_2=19.6 mm, a_3=19.6 mm, a_4=15.6 mm and a_5=5.0 mm for the widths, b_1=5.0 mm, b_2=15.6 mm, b_3=19.6 mm, b_4=19.6 mm and b_5=12.2 mm for the heights, l_1=5.3 mm, l_2=4.0 mm, l_3=8.6 mm, l_4=4.0 mm and l_5=5.3 mm for the lengths. The input and output coupling windows are centered with regard to the central cavity.
The analysis (see Fig. 7) was performed with 150 basis functions and 800 terms in the series (Z matrix), 20 accesible modes and 100 poles in the last cascade connection. Our results (solid lines) are well compared with those provided by the commercial software HFSS (circles). The same accurate results (see stars in Fig. 7) can be obtained if the frequency-by-frequency (point-to-point) technique for cascading Z matrices is used. However, our novel analysis method provides such results in only 1.13 s for 301 frequency points, whereas the

CPU effort is raised to 2.93 s when using the point-to-point connection technique. Finally, the combination of the original integral equation technique with the cited point-to-point connection technique would provide the same accurate results in 29 s. Regarding HFSS, the CPU time was of 467 s (fast sweep).

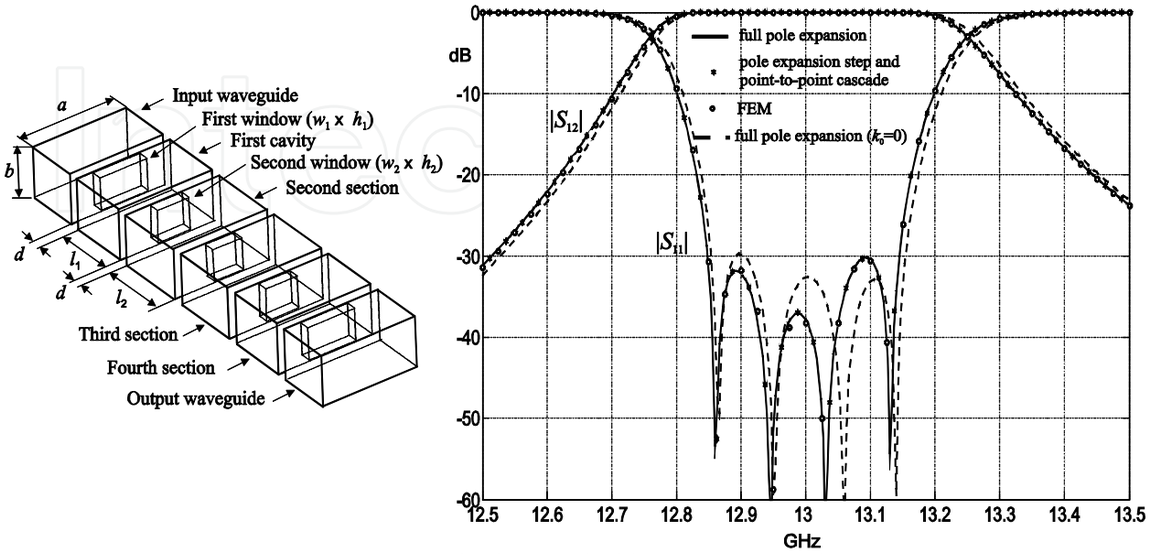

Fig. 6. Geometry and *S* parameters of a four pole filter in rectangular waveguide technology.

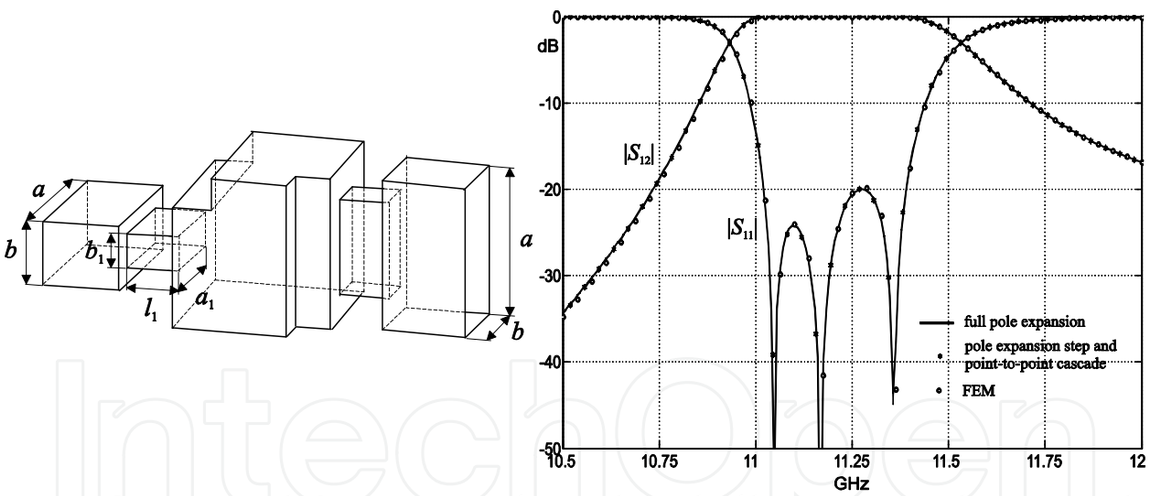

Fig. 7. Geometry and *S* parameters of a triple-mode filter in rectangular waveguide technology.

Next, we have studied the accuracy of the proposed method when used to predict the out-of-band response of the triple-mode filter just considered before. In Fig. 8, we compare the *S* parameters of such structure in a very wide frequency band (1000 points comprised between 8 and 18 GHz) when k_0 in (7) and (107) is chosen to be 0 and equal to the value of the in-band center frequency. As it can be observed, both results are less accurate at very high frequencies (far from the center frequency of the filter), and more accuracy is preserved when additional terms are considered in (107), i.e. when $k_0 \neq 0$. In order to recover more accurate results, even at very high frequencies, it has been needed to increase the number of

accessible modes to 25 and the total number of poles to 250, thus involving a CPU effort (1000 points) of 4.9 s.

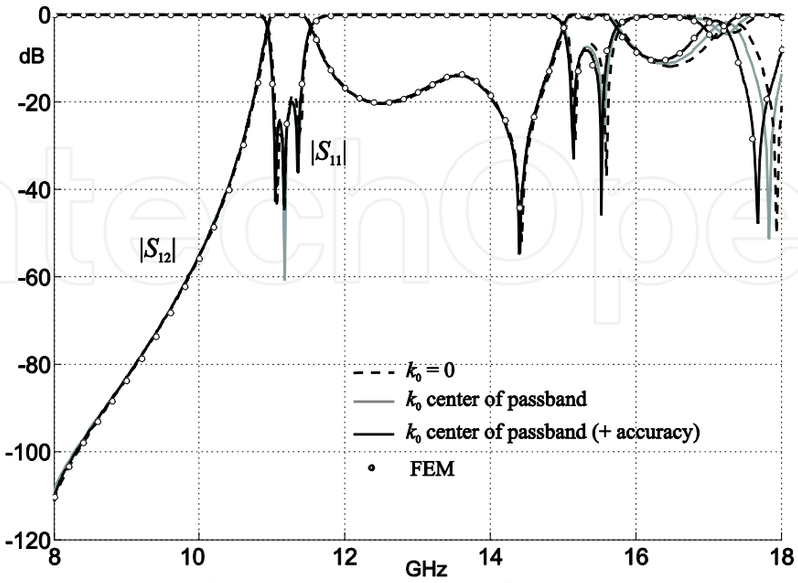

Fig. 8. Out-of-band response of the triple-mode cavity filter.

Now, we apply our novel technique to the analysis of H-plane filters. We have first solved the full-wave analysis of a symmetrical 8-pole inductive filter in WR-137 waveguide (a=34.85 mm, b=15.85 mm), whose topology is included in Fig. 9. The dimensions of the first half (symmetric structure) of coupling windows (with thickness always equal to 2.0 mm) are w_1=22.04 mm, w_2=16.33 mm, w_3=14.59 mm, w_4=14.12 mm and w_5=14.03 mm, and of the cavities are l_1=24.34 mm, l_2=28.31 mm, l_3=29.38 mm and l_4=29.65 mm. The analysis was performed taking into account the symmetries, where N=4 accessible modes were considered for each cascade connection. The waveguide steps were computed with 30 basis functions, and 150 terms in the series. The final number of poles for the whole filter was 60.

In Fig. 9, we successfully compare the S parameters provided by our pole expansion technique (solid lines) with the results obtained by the commercial software HFSS (circles) and by a traditional frequency-by-frequency cascade connection (stars). The CPU effort required by such traditional approach to compute the electrical response for 301 frequency values was equal to 0.26 s, whereas the method proposed in this paper only needed 0.09 s. Regarding the results obtained with HFSS, for an optimal convergence we employed a mesh with 67026 tetrahedra with a CPU time of 56 s for each frequency point.

The second example under consideration is an H-plane dual-mode filter topology proposed in (Guglielmi et al., 2001), whose geometry can be seen in Fig. 10. The input and output sections of this filter are WR-75 waveguides, and the widths and lengths of the three coupling windows are, respectively, w_1=10.931 mm, w_2=10.782 mm and w_3=10.956 mm, d_1=3.0 mm, d_2=12.481 mm and d_3=3.0 mm. The first and last coupling windows are centered, respectively, with regard to the input and output waveguide sections, whereas the offsets between the apertures and the upper walls of the cavities are o_1=18.146 mm, o_2=18.295 mm, o_3=17.915 mm and o_4=18.101 mm. As regards the two resonant cavities of this filter, their widths and lengths are, respectively, a_1=30.077 mm, a_2=29.567 mm, l_1=28.306 mm and l_2=28.852 mm.

The selected configuration for this filter was 5 accessible modes, 60 basis functions, 300 terms in the series and 25 poles after the last cascade connection. Fig. 10 shows our results (solid lines) with those provided by the commercial software HFSS (circles) and by a point-to-point connection technique (stars). Our novel analysis method provides accurate results in only 0.11 s for 301 frequency points, whereas the CPU effort is raised to 0.22 s when using the point-to-point connection technique. The simulation with HFSS was performed with 236994 tetrahedra due to the high sensitivity of this filter, and the CPU time was 279 s for each frequency point. Finally, the results obtained when k_0=0 in (33) and (107) are shown in Fig. 10. As it should be expected, the results computed with such approach converge more slowly than those obtained with our wideband analysis method.

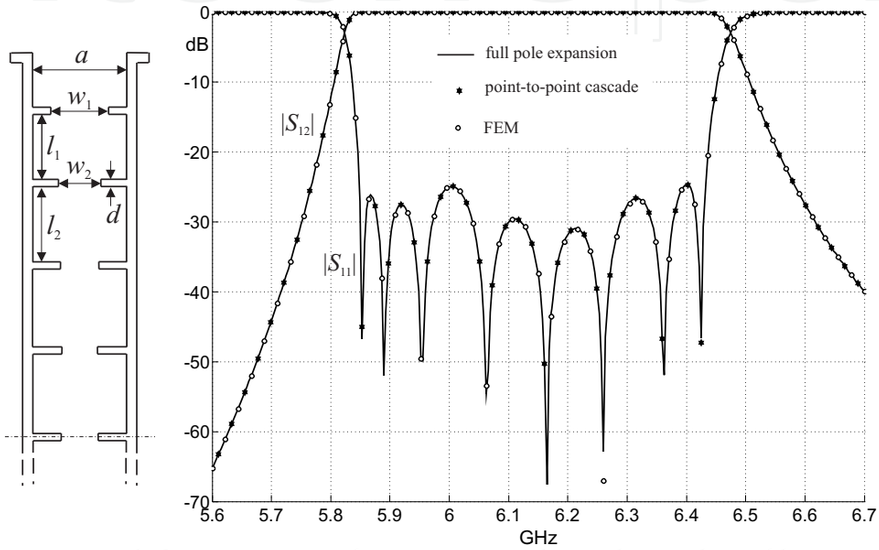

Fig. 9. Geometry and *S* parameters of a symmetrical 8-pole H-plane filter in rectangular waveguide technology.

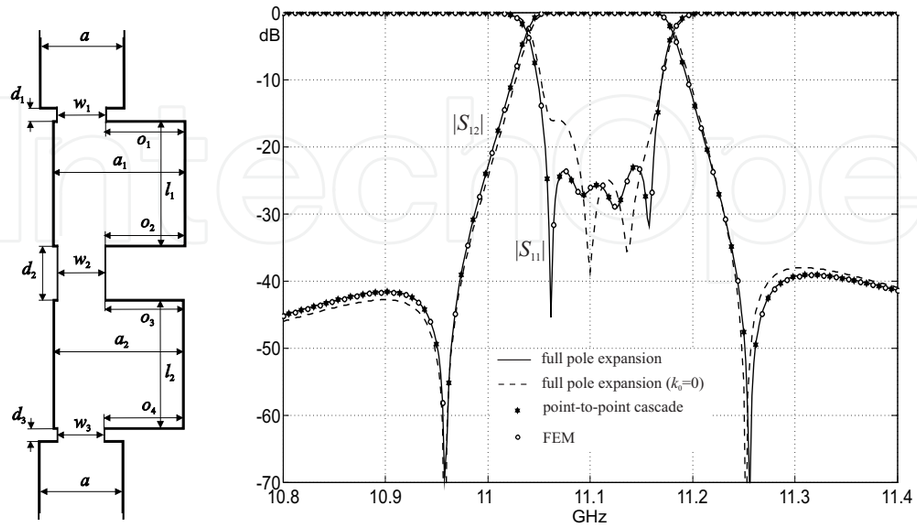

Fig. 10. Geometry and *S* parameters of an H-plane dual-mode filter in rectangular waveguide technology.

The proposed method has been also applied to predict the out-of-band response of the dual-mode filter just considered before. In Fig. 11, we compare the S parameters of such structure in a very wide frequency band (1000 points comprised between 8 and 18 GHz) when k_0 is chosen to be 0 and equal to the value of the in-band center frequency. As it can be observed, both results are slightly less accurate at very high frequencies (far from the center frequency of the filter), and more accuracy is preserved when additional terms are considered in (107), i.e. when $k_0 \neq 0$. In order to recover very accurate results in a very wide frequency band, it has been needed to increase the total number of poles to 75, thus involving a global CPU effort (1000 points) of 0.39 s.

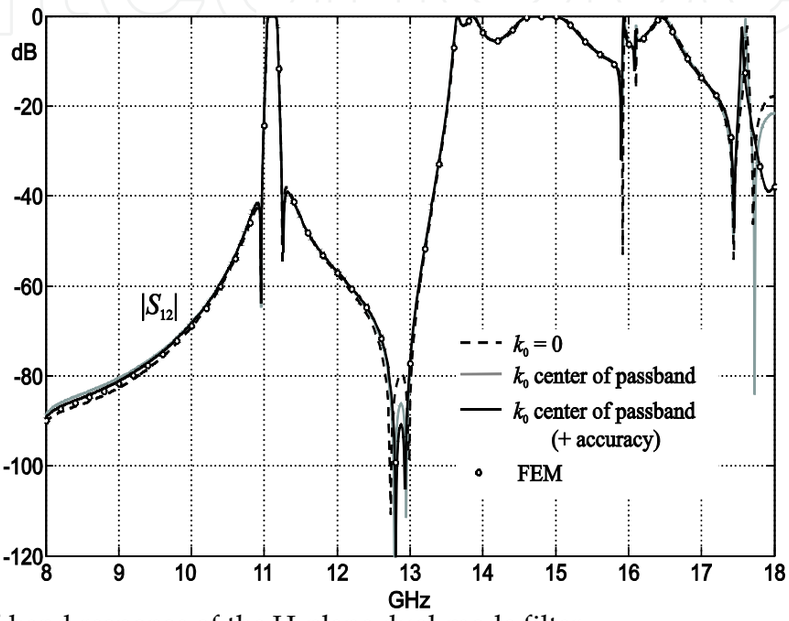

Fig. 11. Out-of-band response of the H-plane dual-mode filter.

7. Conclusions

In this chapter, we have presented a very efficient procedure to compute the wideband generalized impedance and admittance matrix representations of cascaded planar waveguide junctions, which allows to model a wide variety of real passive components. The proposed method provides the generalized matrices of waveguide steps and uniform waveguide sections in the form of pole expansions. Then, such matrices are combined following an iterative algorithm, which finally provides a wideband matrix representation of the complete structure. Proceeding in this way, the most expensive computations are performed outside the frequency loop, thus widely reducing the computational effort required for the analysis of complex geometries with a high frequency resolution. The accuracy and numerical efficiency of this new technique have been successfully validated through the full-wave analysis of several waveguide filters.

With regard to the ananlysis of single waveguide steps, the Z matrix representation offers a better computational efficiency than the Y matrix representation. However, our novel techniche for the admittance case can even provide a better performance than the original integral equation formulated in terms of the Z matrix. The Y matrix represention is useful

when the devices under study include building blocks (i.e. arbitrarily shaped 3D cavities) whose analysis through the BI-RME method typically provides admittance matrices. In this way, a wideband cascade connection of *Y* matrices can be applied.

8. References

Alessandri, F., G. Bartolucci, and R. Sorrentino (1988), Admittance matrix formulation of waveguide discontinuity problems: Computer-aided design of branch guide directional couplers, *IEEE Trans. Microwave Theory Tech.*, *36*(2), 394-403.

Alessandri, F., M. Mongiardo, and R. Sorrentino (1992), Computer-aided design of beam forming networks for modern satellite antennas, *IEEE Trans. Microwave Theory Tech.*, *40*(6), 1117-1127.

Alvarez-Melcón, A., G. Connor, and M. Guglielmi (1996), New simple procedure for the computation of the multimode admittance or impedance matrix of planar waveguide junctions, *IEEE Trans. Microwave Theory Tech.*, *44*(3), 413-418.

Arcioni, P., and G. Conciauro (1999), Combination of generalized admittance matrices in the form of pole expansions, *IEEE Trans. Microwave Theory Tech.*, *47*(10), 1990-1996.

Arcioni, P., M. Bressan, G. Conciauro, and L. Perregrini (1996), Wideband modeling of arbitrarily shaped E-plane waveguide components by the boundary integral-resonant mode expansion method, *IEEE Trans. Microwave Theory Tech.*, *44*(11), 2083-2092.

Arcioni, P., M. Bozzi, M. Bressan, G. Conciauro, and L. Perregrini (2002), Frequency/time-domain modeling of 3D waveguide structures by a BI-RME approach, *Int. Journal of Numer. Modeling: Electron. Networks, Devices and Fields*, *15*(1), 3-21.

Boria, V. E., and B. Gimeno (2007), Waveguide filters for satellites, *IEEE Microwave Magazine*, *8*(5), 60-70.

Boria, V. E., G. Gerini, and M. Guglielmi (1997), An efficient inversion technique for banded linear systems, in *IEEE MTT-S Int. Microw. Symp. Digest*, pp. 1567-1570, Denver.

Conciauro, G., P. Arcioni, M. Bressan, and L. Perregrini (1996), Wideband modelling of arbitrarily shaped H-plane waveguide components by the boundary integral-resonant mode expansion method, *IEEE Trans. Microwave Theory Tech.*, *44*(7), 1057-1066.

Conciauro, G., M. Guglielmi, and R. Sorrentino (2000), *Advanced Modal Analysis - CAD Techniques for Waveguide Components and Filters*, Wiley, Chichester.

Eleftheriades, G., A. Omar, L. Katehi, and G. Rebeiz (1994), Some important properties of waveguide junction generalized scattering matrices in the context of the mode matching technique, *IEEE Trans. Microwave Theory Tech.*, *42*(10), 1896-1903.

Gerini, G., M. Guglielmi, and G. Lastoria (1998), Efficient integral equation formulations for impedance or admittance representation of planar waveguide junction, in *IEEE MTT-S Int. Microw. Symp. Digest*, pp. 1747-1750, Baltimore.

Guillot, P., P. Couffignal, H. Baudrand, and B. Theron, "Improvement in calculation of some surface integrals: Application to junction characterization in cavity filter design", *IEEE Trans. Microwave Theory Tech.*, vol. 41, no. 12, pp. 2156-2160, Dec. 1993.

Gradstheyn, I. S., and I. M. Ryzhik (1980), *Table of Integrals, Series and Products*, Academic Press.

Guglielmi, M., and A. Alvarez-Melcón (1993), Rigorous multimode equivalent network representation of capacitive discontinuities, *IEEE Trans. Microwave Theory Tech.*, *41*(6/7), 1195-1206.

Guglielmi, M., and G. Gheri (1994), Rigorous multimode network representation of capacitive steps, *IEEE Trans. Microwave Theory Tech.*, *42*(4), 622-628.

Guglielmi, M., and G. Gheri (1995), Multimode equivalent network representation of inductive and capacitive multiple posts, *IEE Proc. Microwave Antennas Propag.*, *142*(1), 41-46.

Guglielmi, M., and C. Newport (1990), Rigorous multimode equivalent network representation of inductive discontinuities, *IEEE Trans. Microwave Theory Tech.*, *38*(11), 1651-1659.

Guglielmi, M., G. Gheri, M. Calamia, and G. Pelosi (1994), Rigorous multimode network numerical representation of inductive step, *IEEE Trans. Microwave Theory Tech.*, *42*(2), 317-326.

Gugliemi, M., P. Jarry, E. Kerherve, O. Roquebrum, and D. Schmitt (2001), A new family of all-inductive dual-mode filters, *IEEE Trans. Microwave Theory Tech.*, *49*(10), 1764-1769.

Itoh, T. (1989), *Numerical Techniques for Microwave and Millimeter-Wave Passive Structures*, Wiley, New York.

Lastoria, G., G. Gerini, M. Guglielmi, and F. Emma (1998), CAD of triple-mode cavities in rectangular waveguide, *IEEE Microwave and Guided Wave Letters*, *8*(10), 339-341.

Mansour, R., and R. MacPhie (1986), An improved transmission matrix formulation of cascaded discontinuities and its application to E-plane circuits, *IEEE Trans. Microwave Theory Tech.*, *34*(12), 1490-1498.

Mira, F., A. A. San Blas, V. E. Boria, B. Gimeno, M. Bressan, and L. Perregrini (2006), Efficient pole-expansion of the generalized impedance matrix representation of planar waveguide junctions, in *IEEE MTT-S Int. Microw. Symp. Digest*, pp. 1033-1036, San Francisco.

Safavi-Naini, R., and R. MacPhie (1981), On solving waveguide junction scattering problems by the conservation of complex power technique, *IEEE Trans. Microwave Theory Tech.*, *29*(4), 337-343.

Safavi-Naini, R., and R. MacPhie (1982), Scattering at rectangular-to-rectangular waveguide junctions, *IEEE Trans. Microwave Theory Tech.*, *30*(11), 2060-2063.

Sorrentino, R. (1989), *Numerical Methods for Passive Microwave and Millimeter-Wave Structures*, IEEE Press, New York.

Spiegel, M. R. (1991), *Complex Variables*, Mc Graw-Hill.

Uher, J., J. Bornemann, and U. Rosenberg (1993), *Waveguide Components for Antenna Feed Systems: Theory and CAD*, Artech-House, Norwood.

Wexler, A. (1967), Solution of waveguide discontinuities by modal analysis, *IEEE Trans. Microwave Theory Tech.*, *15*(9), 508-517.

Zhang, F., *Matrix Theory*, Springer-Verlag, New York, 1999.

Microwave and Millimeter Wave Technologies Modern UWB antennas and equipment

Edited by Igor Mini

ISBN 978-953-7619-67-1
Hard cover, 488 pages
Publisher InTech
Published online 01, March, 2010
Published in print edition March, 2010

How to reference

In order to correctly reference this scholarly work, feel free to copy and paste the following:

Fermin Mira, Angel A. San Blas, Vicente E. Boria and Benito Gimeno (2010). Wideband Representation of Passive Components Based on Planar Waveguide Junctions, Microwave and Millimeter Wave Technologies Modern UWB antennas and equipment, Igor Mini (Ed.), ISBN: 978-953-7619-67-1, InTech, Available from: http://www.intechopen.com/books/microwave-and-millimeter-wave-technologies-modern-uwb-antennas-and-equipment/wideband-representation-of-passive-components-based-on-planar-waveguide-junctions

INTECH
open science | open minds

InTech Europe
University Campus STeP Ri
Slavka Krautzeka 83/A
51000 Rijeka, Croatia
Phone: +385 (51) 770 447
Fax: +385 (51) 686 166
www.intechopen.com

InTech China
Unit 405, Office Block, Hotel Equatorial Shanghai
No.65, Yan An Road (West), Shanghai, 200040, China
中国上海市延安西路65号上海国际贵都大饭店办公楼405单元
Phone: +86-21-62489820
Fax: +86-21-62489821

IntechOpen